Gene Expression, Vol. 13, pp. 107–132
Printed in the USA.

1052-2166/06 $90.00 + .00
E-ISSN 1555-3884
www.cognizantcommunication.com

Global Gene Expression Profiling of Dimethylnitrosamine-Induced Liver Fibrosis: From Pathological and Biochemical Data to Microarray Analysis

LI-JEN SU,*† SHIH-LAN HSU,‡ JYH-SHYUE YANG,‡ HUEI-HUN TSENG,§ SHIU-FENG HUANG,§ AND CHI-YING F. HUANG*†§¶#

**Graduate Institute of Life Sciences, National Defense Medical Center, Taipei 114, Taiwan*
†National Institute of Cancer Research, National Health Research Institutes, Taipei 114, Taiwan
‡Department of Education and Research, Taichung Veterans General Hospital, Taichung 407, Taiwan
§Division of Molecular and Genomic Medicine, National Health Research Institutes, Miaoli County 350, Taiwan
¶Institute of Biotechnology in Medicine, National Yang-Ming University, Taipei 112, Taiwan
#Department of Computer Science and Information Engineering, National Taiwan University, Taipei 106, Taiwan

The development of hepatocellular carcinoma (HCC) is generally preceded by cirrhosis, which occurs at the end stage of fibrosis. This is a common and potentially lethal problem of chronic liver disease in Asia. The development of microarrays permits us to monitor transcriptomes on a genome-wide scale; this has dramatically speeded up a comprehensive understanding of the disease process. Here we used dimethylnitrosamine (DMN), a nongenotoxic hepatotoxin, to induce rat necroinflammatory and hepatic fibrosis. During the 6-week time course, histopathological, biochemical, and quantitative RT-PCR analyses confirmed the incidence of necroinflammatory and hepatic fibrosis in this established rat model system. Using the Affymetrix microarray chip, 256 differentially expressed genes were identified from the liver injury samples. Hierarchical clustering of gene expression using a gene ontology database allowed the identification of several stage-specific characters and functionally related clusters that encode proteins related to metabolism, cell growth/maintenance, and response to external challenge. Among these genes, we classified 44 potential necroinflammatory-related genes and 62 potential fibrosis-related markers or drug targets based on histopathological scores. We also compared the results with other data on well-known markers and various other microarray datasets that are available. In conclusion, we believe that the molecular picture of necroinflammatory and hepatic fibrosis from this study may provide novel biological insights into the development of early liver damage molecular classifiers than can be used for basic research and in clinical applications. A public accessible website is available at http://LiverFibrosis.nchc.org.tw:8080/LF.

Key words: Dimethylnitrosamine; Histopathology; Necroinflammatory; Fibrosis; Biochemical data; Microarray; Quantitative RT-PCR; *Tgfb1*; *Timp1*; *Spp1*

INTRODUCTION

Liver fibrosis and cirrhosis, which appear during the end stage of fibrosis, are the major risk factors of hepatocellular carcinoma (HCC). Although a range of factors, such as hepatitis B virus (HBV), hepatitis C virus (HCV), hepatotoxins, metabolic disorders, and alcoholism, can induce liver cirrhosis, hepatic fibrogenesis is also induced by these risk factors and shares a similar phenotype (4,8,20,23,39). However,

Address correspondence to Chi-Ying F. Huang, National Institute of Cancer Research, National Health Research Institutes, 9F Room 9320, No. 161, Sec. 6, Min-Chuan East Road, Taipei 114, Taiwan. Tel: (886)-2-26534401, ext. 25180 or 25181; Fax: (886)-2-2792-9654; E-mail: chiying@nhri.org.tw

it is not clear what types of genes are involved or how they act when liver injury takes place and is repaired. Moreover, the cirrhosis caused by these risk factors often progresses insidiously. Patients with end-stage liver cirrhosis usually die unless they accept liver transplantation, which has a 5-year survival rate of 75% (23).

Previous biochemical studies have reported that there are 39 well-known fibrosis or cirrhosis markers (13,19,23) and these include invasive and noninvasive markers. Recently, the development of microarrays, which permit us to monitor transcriptomes on a genome-wide scale, has dramatically expedited a comprehensive understanding of gene expression profiles and this includes how the transcription profiles for genes vary across the progressive of a disease's development. Moreover, the application of microarray may ultimately reveal unique and identifiable signatures, which are essential to the discovery of new insights into the mechanisms common to, for example, liver fibrosis. Recently, two microarray studies have been carried out that relate to liver fibrosis and cirrhosis. Firstly, liver fibrosis was induced in rats by continuous administration of thioacetamide (TAA) in the drinking water for 12 weeks. The liver samples at a single time point (14th week) were subjected to the Agilent Rat cDNA microarray analysis (45). Secondly, Kim and his colleagues identified 556 chronic liver disease (CLD)-related genes, which included 273 HCC-associated gene signatures and 283 etiology-associated signatures; this involved a comparison of low-risk and high-risk CLD groups using an Incyte human cDNA microarray (26). Thirdly, it is well known that the liver regenerates in response to a variety of injuries (10,34). Rodent partial hepatectomy has been a useful tool and model with which to investigate the signals that regulate the regenerative response. White and his colleagues used a microarray strategy to identify a total of 640 different expression pattern genes that are involved in the hepatic regenerative response (50).

Several animal models have been established to study liver fibrosis (7,17,40,45). In this study, we employed dimethylnitrosamine (DMN), which is a potent nongenotoxic hepatotoxin, to simulate liver fibrosis (16,37) and to perform a 6-week time course Affymetrix microarray study. DMN has been demonstrated to induce liver damage rapidly and also has been empirically proven to be useful for the study of early human fibrosis formation (1,14,25). Moreover, the implementation of histopathological grading of each rat and a statistical approach allows quantitative depiction of the transcriptional regulation during liver fibrosis over a time course. The expression patterns enabled us to identify 256 differentially expressed genes, including 44 necroinflammatory-related and 62 fibrosis-related genes. Comparison of our dataset with earlier related studies reveals multiple overlapping gene identities and these may potentially serve as markers for fibrosis, cirrhosis, and/or HCC diagnosis. Finally, the histopathological, clinical biochemical, and microarray data are stored at http://LiverFibrosis.nchc.org.tw:8080/LF to allow the scientific community to freely access this invaluable information and knowledge.

MATERIALS AND METHODS

Animal Treatments

DMN-induced liver fibrosis model was performed as previously described (25). Male Sprague-Dawley rats (Slc:SD; Japan SLC, Shizuoka, Japan), weighing 300–350 g, were used in all experiments. To induce hepatic fibrosis over a 6-week time course experiment, the rats were given DMN (Sigma, St. Louis, MO) by IP injection. The chemical was dissolved in normal saline and injected three consecutive days a week at a dose of 6.7 mg/kg per body weight. This is a much lower dosage than the one used in other experiments where the level was 100 mg/kg/day DMN. This higher level is able to cause toxicity in rat liver (47,48). The treatment with DMN lasted for only the first 3 weeks (Fig. 1A). Four to seven rats at each time point for each group were treated with either DMN or with an equal volume of normal saline without DMN as the control. All of these rats (26 DMN-treated rats and 24 control rats) were subjected to biochemical and histopathological analysis. However, only two rats for each group at each time point were subjected to microarray analysis. Rats were weighed and sacrificed on days 11, 18, 25, 32, 39, and 46 and these were designated as weeks 1 through 6 (Fig. 1A).

Serum Biochemical Data

Blood samples, collected from the animals at necropsy, were used to measure serum concentrations or activity of albumin, glutamic oxaloacetic transaminase (GOT), glutamic pyruvic transaminase (GPT), total bilirubin, acid phosphatase (ACP), α-fetoprotein (AFP), blood urea nitrogen (BUN), lactate dehydrogenase (LDH), globulin, prothrombin time (PT), and blood platelets (PLT) using an Hitachi 747 and ACL 3000 clinical chemistry analyzer system (MYCO, Renton, WA) at Taichung Veterans General Hospital, Taiwan.

RNA Extraction, Reverse Transcription, and Quantitative Real-Time Reverse Transcriptase Polymerase Chain Reaction (Q-RT-PCR)

We used the same total RNA samples for both microarray and Q-RT-PCR analyses. RNA preparation and analysis were performed according to the Affymetrix's instructions. Briefly, RNA was subjected to reverse transcription with random hexamer primers and the ThermoScript™ RT-PCR system (Life Technologies, Gaithersburg, MD). The cDNAs also served as templates (diluted 200 times) for Q-PCR using an ABI Prism 7700 sequence detection system with TaqMan® Universal PCR Master Mix kit (Applied Biosystems, Foster City, CA). To standardize the quantization of the selected target genes, 18S small subunit ribosomal RNA (18S rRNA) from each sample served as an internal control and was quantified at the same time as the target genes. The cycle threshold (CT) value of the 18S rRNA was used to normalize the target gene expression, referred to as ΔCT, and this was used to correct differences between samples. The Assays-on-Demand IDs of *Tgfb1*, *Timp1*, and 18S rRNA are Rn00572010_m1, Rn00587558_m1, and Hs99999901_s1 (Applied Biosystems, Foster City, CA).

Microarray Analysis

The quality of the total RNA for microarray analysis was determined using Spectra Max Plus (Molecular Devices) and had an A260/A280 ratio ranging from 1.9 to 2.1. Protocols and reagents for hybridization, washing, and staining followed the Affymetrix instructions (http://www.affymetrix.com/support/technical/manuals.affx). Labeled cRNA was hybridized to the Affymetrix GeneChip Test 3 Array to verify the quality prior to hybridization to the Affymetrix Rat Genome U34A Array.

Data Analysis and Clustering Algorithm

The images were transformed into text files containing intensity information using GeneChip® Operating Software (GCOS, similar to MAS 5.0) developed by Affymetrix. The microarray datasets were then analyzed using GeneSpring® 7.2 software (Silicon Genetics, Redwood City, CA).

Western Blot Analysis

Liver samples were lysed in 50% lysate buffer (20 mM PIPES, pH 7.2, 100 mM NaCl, 1 mM EDTA, 0.1% CHAPS, 10% sucrose, 1 mM Na_3VO_4, 1 mM PMSF, and 10 μg/ml each of leupeptin, aprotinin, chymostatin, and pepstatin) and 50% IP washing buffer (10 mM HEPES, pH 7.6, 2 mM $MgCl_2$, 50 mM NaCl, 5 mM EGTA, 0.1% Triton X-100, and 40 mM β-glycerolphosphate) as described previously (51). Protein lysates (50 μg) were resolved by SDS-PAGE on 12% acrylamide gels (Bio-Red, Hercules, CA). Proteins were transferred to PVDF membranes and detected with antibodies by Western blotting analysis. The antibodies used secreted phosphoprotein 1 (Spp1; 1:1000) (R&D Systems) and β-actin (Actb; 1:2500) (Sigma). Bound antibodies were detected by incubation with horseradish-phosphatase conjugated secondary antibodies at 1:3000 for 1 h followed by washing and staining with a Western Lighting™ solution (PerkinElmer Life Sciences, Boston, MA).

Histopathological Examination

The scoring system, modified from the scoring system of the Histology Activity Index (HAI) (24, 27), includes necroinflammatory, fibrosis, and fatty change. Briefly, liver samples were immediately removed after sacrifice. The fixed liver samples were then processed for paraffin embedding. Sections (5 μm) were prepared for hematoxylin and eosin staining (to score necroinflammatory and fatty changes) and for Sirius red/fast green collagen staining (to score for fibrosis) (29). To examine the intensity of the necroinflammatory lesions, each liver sample was first given necrosis and inflammation scores. The grading for necrosis was divided into four scores: normal (N0), mild piecemeal necrosis (N1), bridge necrosis (N2), and confluent necrosis (N3). Similarly, inflammation was also divided into four scores: none (I0), mild (I1), moderate (I2), and marked (I3) according to the intensity of inflammatory cell infiltration at portal areas. The necroinflammatory scores were the sum of the necrosis and inflammation scores and ranged from 0 to 6, designated A0 to A6. In addition, fibrosis was divided into four scores: normal (F0), fibrous expansion of portal tracts (F1), bridging fibrosis (F2), and frequent bridging fibrosis with focal nodule formation (F3). The fatty changes were classified as presence or absence (+/–). There were 4–7 rats per treatment per week. Three represented images of each histology sample section (at 100× magnification) of each rat were selected randomly and have been deposited on a public accessible website (http://LiverFibrosis.nchc.org.tw:8080/LF).

Statistical Analysis

All statistical analyses were performed by SAS/STAT 8e (SAS Institute, Cary, NC). The biochemical data were expressed as mean ± SD. Two-way analysis of variance (ANOVA) was used to build an explicit model about the sources of variances that affect

the measurements. The relationship between the experimental chips was analyzed by linear regression. The similarity between Q-RT-PCR and microarray data of *Timp1* was analyzed by Pearson's correlation coefficients. The differentially regulated genes from microarray data were identified based on the Student's *t*-test at the 1% significance level. Furthermore, the necroinflammatory and fibrosis associated genes were calculated by statistic analysis. Least squares means (LSM), separately estimated for each three-subgroup variation according to necroinflammatory score, were used for the necroinflammatory-related analysis. The Student's *t*-test was used for the fibrosis-related analysis as it was based on a two-subgroup variation in fibrosis score. A p value of less than 0.05 was considered to be statistically significant.

RESULTS

Establishment of the DMN-Induced Rat Hepatic Fibrosis Model

To monitor the process of liver fibrosis, we set up the DMN-induced rat hepatic fibrosis animal model as described in Materials and Methods. Schematically, this model is shown in Figure 1. Over the timeline of 6 weeks, 26 rats were treated with DMN and 24 rats were treated with saline (4–7 rats for each group at each time point). In agreement with previous observations (14), after 3 weeks of DMN treatment, collagen fiber deposition in rat liver could be observed, along with bile duct proliferation, centrilobular necrosis, bridging fibrosis, and fibrosis surrounding the central veins (see below for a detailed description). To gain additional information about the established animal model, the gene expression profile of tumor growth factor-beta 1 (*Tgfb1*), which is the strongest known inducer of fibrogenesis in the effecter cells of hepatic fibrosis and can stimulate the adipocyte transformation (5,9,15,41), was evaluated. The Q-RT-PCR result showed that a higher level of *Tgfb1* mRNA expression was observed in DMN-treated rat livers than in the controls (Fig. 1B). These initial examinations warrant further characterization of the DMN-induced rat hepatic fibrosis model.

Clinical Biochemistry Results

The serum of each rat, 50 rats in total, was subjected to various biochemical examinations related to liver damages. These examinations are shown in Table 1. The variable marker values of the control and DMN-treated rats were further divided into three subgroups (first to second week, third to fourth week, and fifth to sixth week) for statistical analysis. The biochemical data of all DMN-treated subgroups showed abnormal values when compared with controls, as illustrated in Table 1. Two-way ANOVA at a 5% significance level was performed to distinguish the various variations (e.g., treatment vs. controls and differences due to the time course) and to estimate the variance of each individual variable in the ANOVA model. The results are shown in Table 2. No significant differences ($p < 0.05$) were present in the baseline values of all parameters evaluated in the control groups (data not shown). When the DMN-treated and controls were compared, there were 10 serum markers that showed significant differences, including albumin, glutamic pyruvic transferase (GPT), glutamic oxaloacetic transferase (GOT), bilirubin, alkaline phosphatase (AKP), α-fetoprotein (AFP), cholesterol (CHOL), blood urea nitrogen (BUN), prothrombin time (PT), and platelet count (PLT). These differences were not due to changes over the time course (1–6 weeks). In contrast, two-way ANOVA analysis indicated that the time course showed an effect on lactate dehydrogenase (LDH), globulin, and acid phosphatase (ACP). Taken together, the biochemical data for the DMN-treated group suggest that there were changes in many serum markers and that the protein expression levels or physical responses are similar to liver damage phenotypes in human (21,28).

Gene Expression Profiling During DMN-Induced Liver Damage

Over the 6-week time course experiment, the liver samples of 12 controls and 12 DMN-treated rats (2 rats for each time point) were selected and microarray experiments performed on them. Before any statistical analyses were applied to the microarray data, reproducibility was assessed. Genes were selected as present when they were assigned a present call according to the perfect match (PM)/mismatch (MM) algorithm of Affymetrix in all gene chips (31). Of the 8799 probe sets analyzed, overall expression patterns for 2385 transcripts on the chips were reported to be present ($p < 0.04$). To verify that intrasample variability did not obscure differences between the controls and DMN-treated groups, as well as to determine the fold change that we should consider to be significant, we compared the expression profiles among the 24 control datasets. Scatter graphs of expression levels of the 2385 transcripts represented on the microarray were compared with each other. Figure 2A shows the duplicate samples at week 4. Overall, there was no statistical difference at all, with 3.2% of the transcripts deviated more than twofold.

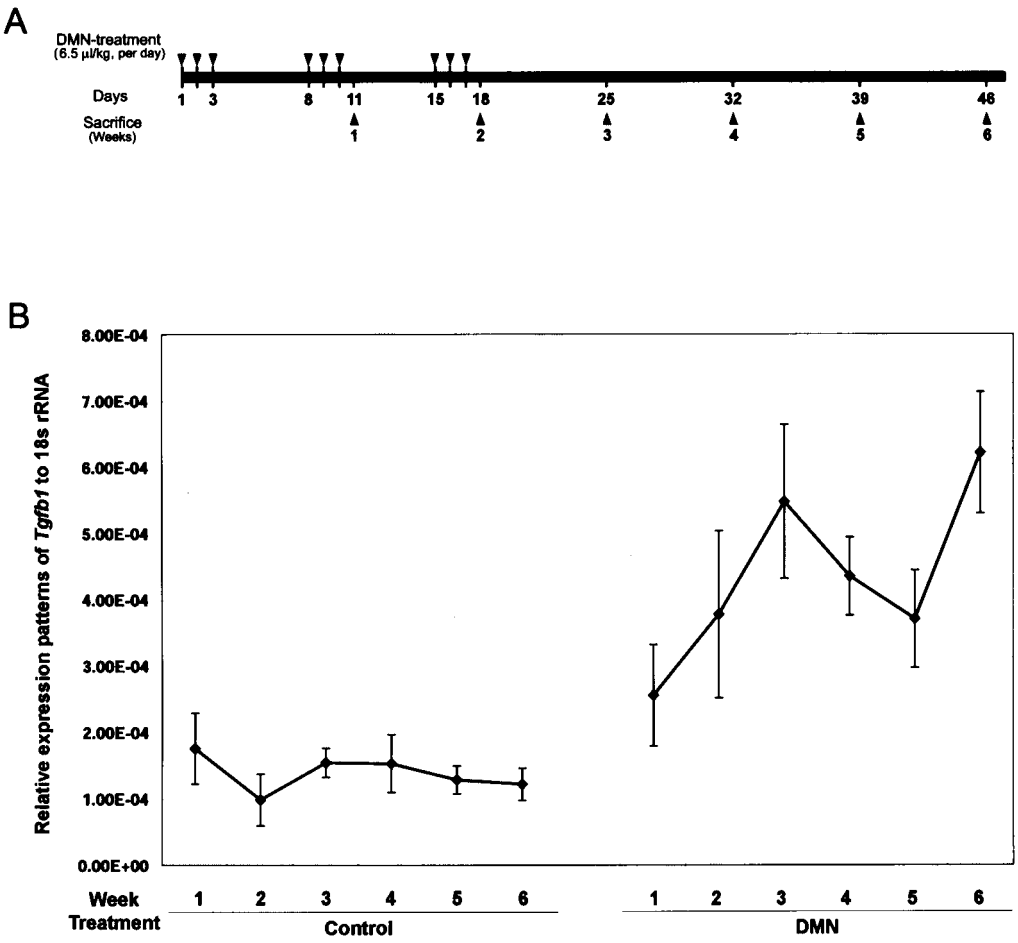

Figure 1. A schematic illustration of DMN-induced fibrosis in rats. (A) Each rat was either injected with DMN three times per week for 3 consecutive weeks (triangle) or injected with normal saline as a control under the same regime. Rats were weighed and sacrificed each week (starting on day 11, which are referred to as first week to sixth week). Blood samples were collected for biochemical assay (summary in Table 1) and livers were excised and weighed, followed by either fixing in formaldehyde for histopathology or isolation of RNA for microarray analysis. (B) The quantitative real-time PCR result for *Tgfb1*. The TaqMan® assays were conducted in triplicate for each sample, and a mean value was used for calculation of expression levels. To standardize the quantification of the target genes, 18S rRNA from each sample was quantified at the same time as the target genes.

To investigate the time course variability, the reliable signals of these 2385 probe sets between the first and sixth week of controls were calculated. Again, they were no statistically difference, with 4.6% of the transcripts deviated more than twofold (Fig. 2B). In contrast, a significant scatter was found between controls and DMN-treated groups, with 28.7% of the transcripts deviated more than twofold (Fig. 2C).

We further investigated whether the controls and DMN-treated groups could be classified into groups on the basis of their gene expression profiles. As the first step to minimize the likelihood of false positives, we filtered all transcripts by forming two independent clusters from the microarray data and identified those that were potentially differentially expressed (Fig. 3). For detailed analysis, the first cluster generated 2385 transcripts as previous described. Of these, 268 were differentially expressed transcripts either higher or lower by 1.5-fold or more when compared with the controls and DMN-treated groups. The second method, which used the "detection flag" selection (31), reported 23 transcripts to be "present" in the DMN-treated groups but not in the controls. In contrast, there was only one transcript reported to be "absent" in all DMN-treated groups but not in the controls. Altogether, 256 genes (or 292 transcripts), including 137 upregulated and 119 downregulated genes, exhibited a differentially expressed gene expression pattern when the DMN-treated groups and controls were compared. Detailed descriptions of all 256 genes including GeneBank ID, name, and fold change are shown in Table 3 and on our liver fibrosis website

TABLE 1
CLINICAL, CHEMICAL, AND FIBROSIS PARAMETERS IN TREATED AND UNTREATED GROUPS OF RATS

	Control			DMN Treatment		
Numeric Variable	1–2 Week (*n*)	3–4 Week (*n*)	5–6 Week (*n*)	1–2 Week (*n*)	3–4 Week (*n*)	5–6 Week (*n*)
Albumin (g/dl)	4.4 ± 0.4 (7)	4.6 ± 0.2 (8)	4.7 ± 0.2 (8)	3.9 ± 0.7 (7)	3.5 ± 0.6 (11)	3.2 ± 0.1 (7)
GPT (U/L)	61.1 ± 26.7 (8)	65.9 ± 19.7 (7)	50.3 ± 4.9 (8)	459.5 ± 78.5 (8)	566.6 ± 313.5 (11)	763.6 ± 405.2 (7)
GOT (U/L)	110.3 ± 37.6 (8)	84.0 ± 23.5 (7)	109.1 ± 23.5 (8)	661.5 ± 134.4 (8)	1006.1 ± 749.6 (11)	1572.9 ± 965.3 (7)
Bilirubin (mg/dl)	0.13 ± 0.05 (8)	0.10 ± 0.01 (8)	0.13 ± 0.05 (8)	0.72 ± 0.53 (8)	1.01 ± 0.74 (11)	1.13 ± 1.00 (7)
AKP (KA)	46.0 ± 3.7 (4)	44.8 ± 2.2 (4)	47.0 ± 13.6 (4)	600.8 ± 93.0 (4)	668.3 ± 222.0 (3)	468 ± 12.7 (2)
LDH (IU/L)	262.3 ± 75.1 (4)	289.3 ± 31.7 (3)	292.3 ± 31.3 (4)	414.8 ± 102.7 (4)	562.0 ± 120.8 (3)	853.5 ± 91.2 (2)
Globulin (g/dl)	6.9 ± 0.3 (3)	6.9 ± 0.5 (4)	7.3 ± 0.2 (4)	6.7 ± 0.1 (2)	5.0 ± 0.8 (4)	3.6 ± 0.3 (2)
Triglyceride (mg/dl)	130 ± 48 (4)	144 ± 8 (4)	170 ± 27 (4)	151 ± 107 (4)	181 ± 144 (7)	103 ± 35 (5)
AFP (ng/dl)	0.32 ± 0.04 (4)	0.2 ± 0.01 (2)	0.24 ± 0.03 (4)	0.40 ± 0.19 (4)	0.38 ± 0.05 (4)	0.35 ± 0.07 (2)
CHOL (mg/dl)	88 ± 5 (4)	71 ± 20 (4)	91 ± 5 (4)	77 ± 8 (4)	70 ± 13 (6)	67 ± 18 (5)
BUN (mg/dl)	31 ± 2 (4)	25 ± 6 (4)	26 ± 9 (4)	33 ± 4 (4)	36 ± 2 (4)	31 ± 5 (2)
ACP (mg/dl)	2.3 ± 0.8 (4)	2.6 ± 0.5 (4)	2.3 ± 0.8 (4)	1.9 ± 0.6 (4)	6.2 ± 1.1 (4)	8.2 ± 0.6 (2)
PT (s)	14 ± 1 (7)	13 ± 1 (8)	13 ± 1 (7)	18 ± 4 (8)	20 ± 4 (9)	22 ± 5 (6)
PLT (10^3/ml)	741 ± 245 (8)	981 ± 124 (8)	893 ± 109 (8)	407 ± 72 (7)	300 ± 165 (11)	229 ± 302 (7)

Values are mean ± SD from 1–2-, 3–4-, or 5–6-week treated and untreated groups. *n*: number of rats. GPT, glutamic pyruvic transaminase; GOT, glutamic oxaloacetic transaminase; bilirubin, total bilirubin; AKP, alkaline phosphatase; LDH, lactate dehydrogenase; AFP, α-fetoprotein; CHOL, cholesterol; BUN, blood urea nitrogen; ACP, acid phosphatase; PT, prothrombin time; PLT, blood platelet.

(see below). Hierarchical clustering generated a dendrogram for the gene expression patterns of these 292 transcripts across the 24 samples as shown in Figure 4A.

These 256 genes were further classified on biological process, molecular function, and cellular component involved based on gene ontology analysis (http://fatigo.bioinfo.cipf.es/) (2). In either category, the largest proportion (approximately 50%) was found to be uncharacterized genes and the summary results are shown in Figure 4B. A hierarchical clustering was further employed to organize each of these top three categories of biological process into a dendrogram (Fig. 4C).

TABLE 2
SUMMARY OF STATISTICAL ANALYSIS OF BIOCHEMICAL DATA

	p-Value of Control or DMN Treatment Groups		
Numeric Variable	Drug	Week	Drug × Week
Albumin (g/dl)	<0.0001*	0.89	0.15
GPT (U/ml)	<0.0001*	0.18	0.13
GOT (U/ml)	<0.0001*	0.055	0.06
Bilirubin	<0.0001*	0.59	0.57
AKP	<0.0001*	0.20	0.19
LDH	<0.0001*	0.005*	0.002*
Globulin	<0.0001*	0.005*	0.0004*
Triglyceride	0.93	0.80	0.41
AFP	0.02*	0.32	0.67
CHOL	0.02*	0.17	0.21
BUN	0.02*	0.50	0.23
ACP	<0.0001*	<0.0001*	<0.0001*
PT	<0.0001*	0.60	0.31
PLT	<0.0001*	0.40	0.02*

Significance was calculated using two-way ANOVA.
*$p < 0.05$ versus untreated group (control).

To validate our microarray data, Q-RT-PCR analysis was performed for tissue inhibitor of metalloproteinase 1 (*Timp1*), tissue inhibitor of metalloproteinase 2 (*Timp2*), matrix metalloproteinase 3 (*Mmp3*), and gamma-glutamyl transpeptidase (*Ggtp*). These genes were chosen for validation because these genes were identified both in this GeneChip study and in previous studies. As determined by Q-RT-PCR, *Timp1* (Fig. 4D), *Timp2*, *Mmp3*, *Ggtp* (data not shown), and *Tgfb1* (shown previously in Fig. 1B) were elevated in DMN-treated samples. The results of Q-RT-PCR analysis of these five genes were consistent with previous reports examining these individual markers (13,19). Moreover, we observed good concordance based on the fold changes between the microarray data and the Q-RT-PCR results. As shown in Figure 4D, *Timp1* expression was elevated over 20-fold in DMN-treated rats in both microarray and Q-RT-PCR. The expression patterns for *Timp1* was highly correlated between the Q-RT-PCR results and the GeneChip analysis (the Pearson's correlation coefficients were 0.79 and 0.92, respectively) (Fig. 4D), suggesting that our gene expression results were reliable when subject to more detailed analysis.

SPP1, secreted phosphoprotein 1 (also known as osteopontin), is a secreted matrix protein. Recently, it has been shown to be overexpressed in metastatic HCC (33). However, it is not known whether the ex-

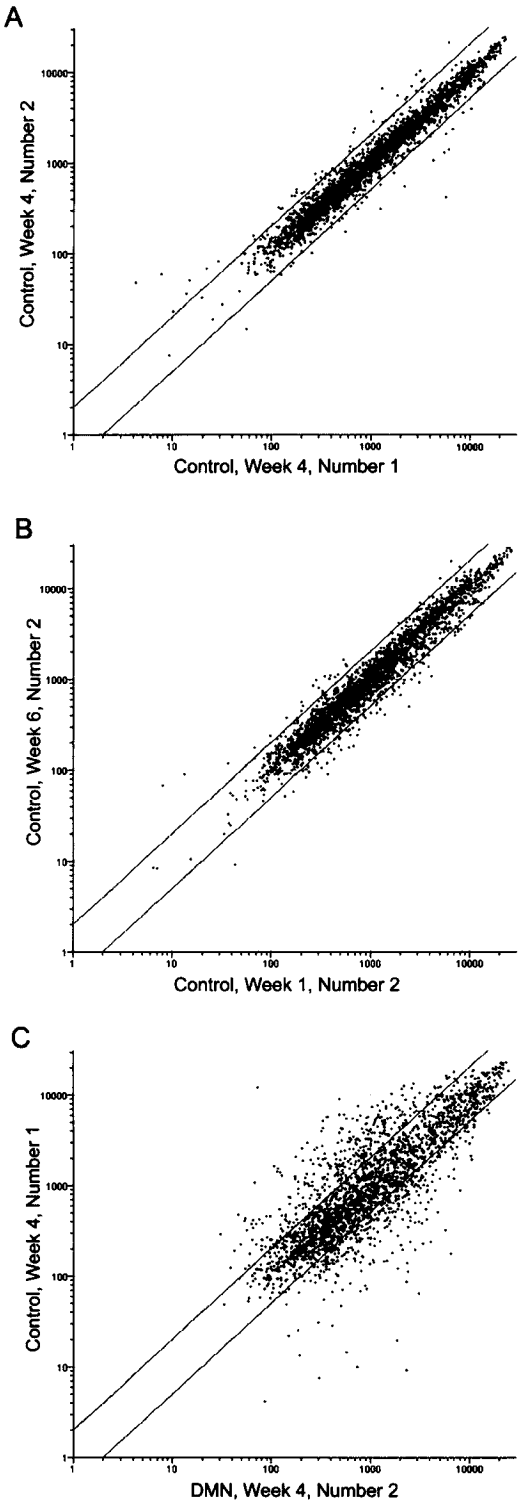

Figure 2. Interactive scatter plot display of the absolute intensity values for the 2385 unique transcripts represented on the Gene Chip. (A) Biological variability of s in the duplicate experiments (C41 and C42); 3.2% of transcripts deviated more than twofold. (B) Biological variability of s from the first versus sixth week (C12 and C62); 4.6% of transcripts deviated more than twofold. (C) Biological variability between the control and DMN-treated rats at the fourth week (C41 and D42); 28.7% of transcripts deviated more than twofold.

pression pattern of SPP1 exhibits any changes during early liver inflammation and fibrosis. Western blotting analysis indicated that protein level of Spp1 was significantly overexpressed after the fourth week of DMN treatment (Fig. 4E), suggesting that Spp1 may be a potential early diagnostic marker for patients with inflammation and fibrosis.

Histopathology Results

To capture the progression of liver damage, a scoring system, as described in detail in Materials and Methods was used to characterize the phenotypic changes as the result of DMN-induced liver damages (Fig. 5A). There are three histopathological gradings in this study, including necroinflammatory (A0–A6), which is the sum of necrosis (N0–N3) and inflamma-

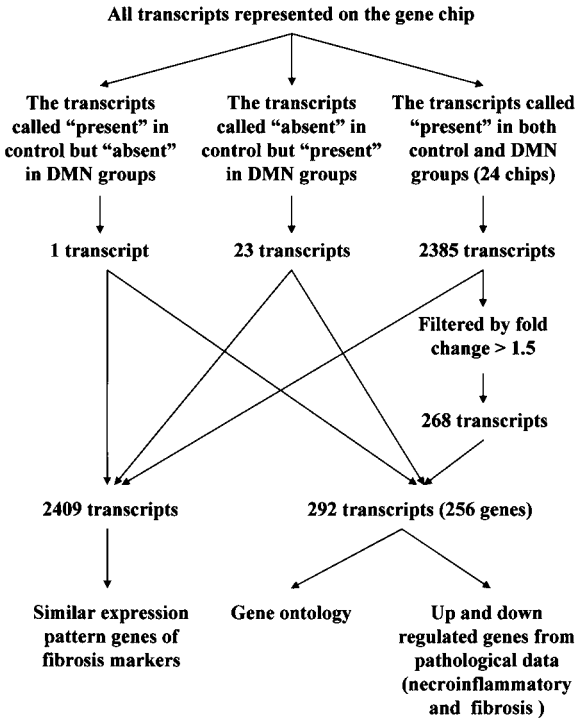

Figure 3. Flowchart of steps for implementation of statistical protocols and our comprehensive cutoff points for data mining. Transcripts (2409) were filtered in control group and DMN-treated group. One and 24 transcripts were clustered as all present in the control but all absent in the DMN-treated group and all present in the DMN-treated but all absent in control group, respectively. In total, 2385 present transcripts were clustered from all 24 chips. All reliable transcripts were found to have similar expression pattern as genes that are well known as fibrosis markers by Pearson correlation ($r > 0.8$). A further 268 transcripts were further filtered as showing a 1.5-fold change from the initial 2385 genes. Two hundred and ninety-two transcripts (256 genes) were identified and subjected to more detailed analysis including gene ontology detection and histopathology (necroinflammatory and fibrosis)-related genes analysis.

TABLE 3
GENES WITH MOST SIGNIFICANT CHANGES IN EXPRESSION BETWEEN TREATED AND UNTREATED GROUPS

GenBank Accession No.	Description	Mean ± SD of Control	Mean ± SD of DMN Treatment	Fold Change	*p*-Value
Downregulated genes					
X14552	Protein phosphatase 2 (formerly 2A), regulatory subunit B (PR 52), alpha isoform	10.58 ± 4.22	0.70 ± 0.29	↓ 15.2	<0.0001
D14564	*Rattus norvegicus* gene for L-gulono-gamma-lactone oxidase, exon 7	3.07 ± 0.69	0.49 ± 0.28	↓ 6.2	<0.0001
M64755	Cysteine-sulfinate decarboxylase	3.26 ± 1.28	0.53 ± 0.29	↓ 6.2	<0.0001
AA893325	Ornithine aminotransferase	4.41 ± 1.12	0.83 ± 0.29	↓ 5.3	<0.0001
M93297	*Rattus norvegicus* ornithine aminotransferase (rOAT) gene, exon 7	4.10 ± 1.51	0.78 ± 0.19	↓ 5.3	<0.0001
AA892345	Rat mRNA for dimethylglycine dehydrogenase (EC number 1.5.99.2)	2.72 ± 0.71	0.53 ± 0.29	↓ 5.1	<0.0001
J05210	ATP citrate lyase	2.93 ± 1.58	0.60 ± 0.33	↓ 4.9	0.00031
AA893552	*Rattus norvegicus* kallistatin mRNA, complete cds	2.70 ± 0.52	0.65 ± 0.27	↓ 4.1	<0.0001
M00002	Apolipoprotein A-IV	2.99 ± 1.34	0.75 ± 0.31	↓ 4.0	<0.0001
D00362	*Rattus norvegicus* mRNA for carboxyesterase E1, partial cds	1.33 ± 0.24	0.33 ± 0.24	↓ 4.0	<0.0001
AI232087	Hydroxyacid oxidase 3 (medium-chain)	2.43 ± 0.52	0.62 ± 0.34	↓ 3.9	<0.0001
X52625	3-Hydroxy-3-methylglutaryl-Coenzyme A synthase 1	2.65 ± 0.77	0.69 ± 0.27	↓ 3.8	<0.0001
S49003	Short isoform growth hormone receptor (rats, mRNA, 1136 nt)	1.93 ± 0.42	0.52 ± 0.23	↓ 3.7	<0.0001
M22359	Alpha(1)-inhibitor 3, variant I	2.12 ± 1.03	0.57 ± 0.43	↓ 3.7	0.00024
AF038870	Betaine-homocysteine methyltransferase	2.04 ± 0.30	0.55 ± 0.24	↓ 3.7	<0.0001
H31813	ESTs, moderately similar to T14781 hypothetical protein DKF-Zp586B1621.1 (*H. sapiens*)	1.92 ± 0.59	0.55 ± 0.29	↓ 3.5	<0.0001
M59861	10-Formyltetrahydrofolate dehydrogenase	1.86 ± 0.37	0.54 ± 0.28	↓ 3.5	<0.0001
M77479	Solute carrier family 10 (sodium/bile acid cotransporter family), member 1	1.66 ± 0.45	0.48 ± 0.36	↓ 3.4	<0.0001
M22993	Alpha(1)-inhibitor 3, variant I	2.32 ± 1.84	0.69 ± 0.45	↓ 3.3	0.01129
U32314	Pyruvate carboxylase	1.88 ± 0.40	0.57 ± 0.31	↓ 3.3	<0.0001
AA891774	ESTs, similar to RIKEN cDNA 1810013B01	1.76 ± 0.28	0.54 ± 0.24	↓ 3.3	<0.0001
U39206	*Rattus norvegicus* cytochrome P450 4F4 (CYP4F4) mRNA, complete cds	1.87 ± 0.44	0.58 ± 0.40	↓ 3.2	<0.0001
M16235	Lipase, hepatic	1.74 ± 0.40	0.55 ± 0.28	↓ 3.2	<0.0001
AF097723	Plasma glutamate carboxypeptidase	1.86 ± 0.30	0.60 ± 0.24	↓ 3.1	<0.0001
M26127	Rat cytochrome P-450 ISF/BNF-G mRNA	1.76 ± 0.46	0.57 ± 0.38	↓ 3.1	<0.0001
AA893032	ESTs, NAD(P) dependent steroid dehydrogenase-like	1.70 ± 0.46	0.55 ± 0.28	↓ 3.1	<0.0001
D90109	Fatty acid Coenzyme A ligase, long chain 2	1.65 ± 0.37	0.54 ± 0.28	↓ 3.1	<0.0001
AA926193	Sulfotransferase family, cytosolic, 1C, member 2	1.81 ± 0.35	0.60 ± 0.31	↓ 3.0	<0.0001
U10697	Carboxylesterase 1	1.70 ± 0.37	0.57 ± 0.32	↓ 3.0	<0.0001
X76456	Unnamed protein product; *R. norvegicus* (Sprague Dawley) alpha albumin gene	1.72 ± 0.52	0.58 ± 0.26	↓ 2.9	<0.0001
AA893244	ESTs, 3′-phosphoadenosine 5′-phosphosulfate synthase 2 (predicted)	2.20 ± 0.54	0.75 ± 0.24	↓ 2.9	<0.0001
AA893495	ESTs, highly similar to CORTICOSTEROID-BINDING GLOBULIN PRECURSOR (*R. norvegicus*)	1.52 ± 0.32	0.52 ± 0.33	↓ 2.9	<0.0001
U72497	Fatty acid amide hydrolase	1.84 ± 0.32	0.63 ± 0.21	↓ 2.9	<0.0001
S46785	Insulin-like growth factor binding protein complex acid-labile subunit (rats, liver, mRNA, 2190 nt)	1.91 ± 0.50	0.66 ± 0.38	↓ 2.9	<0.0001
D00752	Serine protease inhibitor	1.60 ± 0.34	0.55 ± 0.31	↓ 2.9	<0.0001
AA859994	ESTs, cDNA clone IMAGE:7308494	1.85 ± 0.51	0.64 ± 0.16	↓ 2.9	<0.0001
U68168	Kynureninase (L-kynurenine hydrolase)	1.81 ± 0.48	0.64 ± 0.41	↓ 2.8	<0.0001
AA817846	3-Hydroxybutyrate dehydrogenase (heart, mitochondrial)	1.63 ± 0.43	0.57 ± 0.38	↓ 2.8	<0.0001
AF080468	Glucose-6-phosphatase, transport protein 1	1.62 ± 0.45	0.58 ± 0.26	↓ 2.8	<0.0001
U39943	*Rattus norvegicus* cytochrome P450 pseudogene (CYP2J3P1) mRNA	1.49 ± 0.20	0.53 ± 0.30	↓ 2.8	<0.0001
AA892916	ESTs, similar to RIKEN cDNA 2310001A20 (predicted)	1.98 ± 0.68	0.71 ± 0.20	↓ 2.8	<0.0001
U04733	Arachidonic acid epoxygenase	1.44 ± 0.26	0.51 ± 0.43	↓ 2.8	<0.0001
AA859645	Attractin	2.11 ± 0.53	0.76 ± 0.20	↓ 2.8	<0.0001
AA859899	ESTs, hypothetical protein XP_379516 (Homo sapiens)	1.67 ± 0.48	0.60 ± 0.23	↓ 2.8	<0.0001
AA799560	N-myc downstream-regulated gene 2	1.55 ± 0.22	0.56 ± 0.30	↓ 2.8	<0.0001
S76489	This sequence comes from Figure 1; estrogen sulfotransferase isoform 3 (rats, male, liver, mRNA, 1000 nt)	1.46 ± 0.21	0.53 ± 0.33	↓ 2.7	<0.0001
M11266	Ornithine carbamoyltransferase	1.55 ± 0.27	0.56 ± 0.28	↓ 2.7	<0.0001

TABLE 3
CONTINUED

GenBank Accession No.	Description	Mean ± SD of Control	Mean ± SD of DMN Treatment	Fold Change	*p*-Value
M67465	Hydroxy-delta-5-steroid dehydrogenase, 3 beta- and steroid delta-isomerase	1.80 ± 0.53	0.66 ± 0.36	↓ 2.7	<0.0001
M13646	*Rattus norvegicus* Sprague Dawley testosterone 6-beta-hydroxylase, cytochrome P450/6-beta-A, (CYP3A2)	1.45 ± 0.43	0.54 ± 0.30	↓ 2.7	<0.0001
AA892234	ESTs, moderately similar to microsomal glutathione *S*-transferase 3 (*H. sapiens*)	1.63 ± 0.20	0.61 ± 0.25	↓ 2.7	<0.0001
U10357	Pyruvate dehydrogenase kinase 2 subunit p45 (PDK2)	1.70 ± 0.34	0.64 ± 0.18	↓ 2.7	<0.0001
J05031	Isovaleryl Coenzyme A dehydrogenase	1.60 ± 0.20	0.61 ± 0.25	↓ 2.6	<0.0001
AF075382	Cytokine inducible SH2-containing protein 2	2.95 ± 1.39	1.13 ± 0.69	↓ 2.6	0.00090
M81183	Rat insulin-like growth factor I gene, 3′ end of exon 6	1.90 ± 0.58	0.73 ± 0.35	↓ 2.6	<0.0001
D28560	Ectonucleotide pyrophosphatase/phosphodiesterase 2	1.41 ± 0.35	0.54 ± 0.36	↓ 2.6	<0.0001
AB002584	Beta-alanine-pyruvate aminotransferase	1.90 ± 0.61	0.74 ± 0.26	↓ 2.6	<0.0001
AA946532	ATP-binding cassette, subfamily D (ALD), member 3	1.74 ± 0.55	0.68 ± 0.17	↓ 2.5	<0.0001
H33491	Phenylalkylamine Ca^{2+} antagonist (emopamil) binding protein	1.67 ± 0.44	0.66 ± 0.19	↓ 2.5	<0.0001
AB008424	Rat cytochrome P-450 IID3 mRNA, complete cds	1.55 ± 0.25	0.61 ± 0.33	↓ 2.5	<0.0001
J02791	Acyl-coenzyme A dehydrogenase, C-4 to C-12 straight-chain	1.67 ± 0.32	0.66 ± 0.31	↓ 2.5	<0.0001
J03588	Guanidinoacetate methyltransferase	1.27 ± 0.24	0.50 ± 0.27	↓ 2.5	<0.0001
Z50144	Kynurenine aminotransferase II	1.65 ± 0.22	0.66 ± 0.41	↓ 2.5	<0.0001
AI172017	Aldehyde dehydrogenase 2, mitochondrial	1.72 ± 0.27	0.69 ± 0.20	↓ 2.5	<0.0001
M11670	Catalase	1.55 ± 0.63	0.62 ± 0.33	↓ 2.5	0.00035
S48325	RLM6; diabetes-inducible cytochrome P450RLM6 (rats, liver, mRNA Partial, 1093 nt)	1.37 ± 0.24	0.55 ± 0.24	↓ 2.5	<0.0001
M23601	Monoamine oxidase B	1.67 ± 0.24	0.67 ± 0.32	↓ 2.5	<0.0001
D85035	Dihydropyrimidine dehydrogenase	1.61 ± 0.34	0.65 ± 0.27	↓ 2.5	<0.0001
L24207	Cytochrome P450, subfamily IIIA, polypeptide 3	1.62 ± 0.48	0.66 ± 0.25	↓ 2.5	<0.0001
X06150	Glycine methyltransferase	1.61 ± 0.41	0.65 ± 0.38	↓ 2.5	<0.0001
J04591	Dipeptidyl peptidase 4	1.50 ± 0.28	0.61 ± 0.21	↓ 2.5	<0.0001
D63704	Dihydropyrimidinase	1.57 ± 0.18	0.64 ± 0.36	↓ 2.4	<0.0001
AA892675	ESTs, weakly similar to T20360 hypothetical protein D2030.9b—*Caenorhabditis elegans* (*C. elegans*)	1.74 ± 0.35	0.72 ± 0.24	↓ 2.4	<0.0001
AA891733	ESTs, normalized rat kidney, Bento Soares *Rattus* sp. cDNA clone RKIAG10 3-end, mRNA sequence	1.68 ± 0.42	0.70 ± 0.18	↓ 2.4	<0.0001
S45663	SC2=synaptic glycoprotein (rats, brain, mRNA, 1178 nt)	1.47 ± 0.31	0.61 ± 0.23	↓ 2.4	<0.0001
AA893235	ESTs, G0/G1 switch gene 2 (predicted)	1.78 ± 0.72	0.75 ± 0.36	↓ 2.4	0.00037
AA799771	ESTs, normalized rat heart, Bento Soares *Rattus* sp. cDNA clone RHEAF15 3-end, mRNA sequence	1.78 ± 0.47	0.75 ± 0.22	↓ 2.4	<0.0001
AI639418	Thyroxine deiodinase, type I	1.47 ± 0.27	0.63 ± 0.27	↓ 2.4	<0.0001
M26594	*Rattus norvegicus* malic enzyme (MAL) gene, exon 14 and complete cds	1.74 ± 1.25	0.75 ± 0.24	↓ 2.3	0.01885
L14323	Phospholipase C-beta1	1.58 ± 0.16	0.68 ± 0.26	↓ 2.3	<0.0001
U17697	Cytochrom P450 Lanosterol 14 alpha-demethylase	1.62 ± 0.62	0.71 ± 0.25	↓ 2.3	0.00028
AI013861	3-Hydroxyisobutyrate dehydrogenase	1.44 ± 0.25	0.63 ± 0.21	↓ 2.3	<0.0001
H33426	ESTs, farnesyl diphosphate farnesyl transferase 1	1.67 ± 0.40	0.73 ± 0.20	↓ 2.3	<0.0001
AF080568	Phosphate cytidylyltransferase 2, ethanolamine	1.66 ± 0.34	0.73 ± 0.26	↓ 2.3	<0.0001
X56228	Thiosulfate sulphurtransferase (rhodanese)	1.35 ± 0.17	0.60 ± 0.31	↓ 2.3	<0.0001
M86235	*Rattus norvegicus* mRNA for ketohexokinase	1.35 ± 0.16	0.60 ± 0.18	↓ 2.3	<0.0001
M12337	Phenylalanine hydroxylase	1.57 ± 0.17	0.70 ± 0.23	↓ 2.2	<0.0001
AI229440	Diaphorase (NADH) (cytochrome b-5 reductase)	1.74 ± 0.37	0.78 ± 0.20	↓ 2.2	<0.0001
M60103	Protein tyrosine phosphatase, receptor-type, F	1.77 ± 0.38	0.80 ± 0.21	↓ 2.2	<0.0001
U94856	Paraoxonase 1	1.33 ± 0.13	0.60 ± 0.27	↓ 2.2	<0.0001
AA799645	FXYD domain-containing ion transport regulator 1	1.70 ± 0.37	0.78 ± 0.28	↓ 2.2	<0.0001
AA892832	ESTs, ELOVL family member 5, elongation of long chain fatty acids (yeast)	1.51 ± 0.31	0.69 ± 0.29	↓ 2.2	<0.0001
M27467	Cytochrome oxidase subunit VIc	1.66 ± 1.12	0.76 ± 0.23	↓ 2.2	0.01813
M33648	Rat mitochondrial 3-hydroxy-3-methylglutaryl-CoA synthase mRNA, complete cds	1.35 ± 0.31	0.63 ± 0.19	↓ 2.2	<0.0001
H31897	ESTs, rat PC-12 cells, untreated *Rattus norvegicus* cDNA clone RPCBC56 3- end, mRNA sequence	1.48 ± 0.32	0.69 ± 0.27	↓ 2.1	<0.0001
J03914	Glutathione *S*-transferase Yb subunit; rat glutathione *S*-transferase Yb subunit gene, complete cds	1.43 ± 0.27	0.67 ± 0.22	↓ 2.1	<0.0001

TABLE 3
CONTINUED

GenBank Accession No.	Description	Mean ± SD of Control	Mean ± SD of DMN Treatment	Fold Change	*p*-Value
K00996	Cytochrome p-450e; rat cytochrome p-450e (phenobarbital-induced) mRNA, 3′ end	1.58 ± 0.44	0.76 ± 0.21	↓ 2.1	<0.0001
AA875050	ESTs, weakly similar to KICE RAT CHOLINE/ETHANOLAMINE KINASE (*R. norvegicus*)	1.23 ± 0.14	0.60 ± 0.21	↓ 2.1	<0.0001
M89945	Rat farnesyl diphosphate synthase gene, exons 1-8	1.33 ± 0.39	0.65 ± 0.30	↓ 2.1	<0.0001
L07736	Carnitine palmitoyltransferase 1 alpha, liver isoform	1.39 ± 0.42	0.68 ± 0.18	↓ 2.0	<0.0001
X12459	Arginosuccinate synthetase 1	1.57 ± 0.22	0.78 ± 0.19	↓ 2.0	<0.0001
S83279	HSD IV=peroxisome proliferator-inducible gene (rats, F344, liver, mRNA partial, 2480 nt)	1.46 ± 0.30	0.73 ± 0.27	↓ 2.0	<0.0001
X64336	Protein C	1.36 ± 0.38	0.68 ± 0.22	↓ 2.0	<0.0001
M13100	Rat long interspersed repetitive DNA sequence LINE3 (L1Rn)	1.48 ± 0.60	0.74 ± 0.25	↓ 2.0	0.00151
M15185	*S*-adenosyl-L-homocysteine hydrolase (EC 3.3.1.1)	1.41 ± 0.27	0.72 ± 0.20	↓ 2.0	<0.0001
AA859980	T-complex 1	1.64 ± 0.52	0.84 ± 0.17	↓ 2.0	0.00020
D13921	Acetyl-Co A acetyltransferase 1, mitochondrial	1.28 ± 0.23	0.65 ± 0.19	↓ 2.0	<0.0001
AB000199	*Rattus norvegicus* cca2 mRNA, complete cds	1.50 ± 0.48	0.77 ± 0.24	↓ 1.9	0.00023
AA866302	4-Hydroxyphenylpyruvic acid dioxygenase	1.46 ± 0.24	0.76 ± 0.22	↓ 1.9	<0.0001
X78855	Organic cation transporter	1.58 ± 0.38	0.82 ± 0.17	↓ 1.9	<0.0001
X16481	Parathymosin	1.41 ± 0.26	0.73 ± 0.18	↓ 1.9	<0.0001
AA892821	Aldo-keto reductase family 7, member A2 (aflatoxin aldehyde reductase)	1.32 ± 0.24	0.70 ± 0.18	↓ 1.9	<0.0001
X55660	Proprotein convertase subtilisin/kexin type 3	1.49 ± 0.36	0.78 ± 0.13	↓ 1.9	<0.0001
AI639504	ESTs, weakly similar to T13607 hypothetical protein EG: 87B1.3—fruit fly (*D. melanogaster*)	1.40 ± 0.31	0.75 ± 0.24	↓ 1.9	<0.0001
AA799762	ESTs, similar to RIKEN cDNA 2700038C09 (predicted)	1.49 ± 0.24	0.80 ± 0.30	↓ 1.9	<0.0001
D85844	Rabaptin 5	1.47 ± 0.14	0.80 ± 0.17	↓ 1.8	<0.0001
L12016	Immature protein; rat tricarboxylate transport protein mRNA, complete cds	1.55 ± 0.32	0.84 ± 0.14	↓ 1.8	<0.0001
AI639097	rx01264s rat mixed-tissue library *Rattus norvegicus* cDNA clone rx01264 3′, mRNA sequence	1.64 ± 0.59	0.89 ± 0.32	↓ 1.8	0.00122
AA945583	Hydroxysteroid (17-beta) dehydrogenase 10	1.31 ± 0.25	0.76 ± 0.15	↓ 1.7	<0.0001
AI639417	ESTs, membrane targeting (tandem) C2 domain containing 1	1.50 ± 0.47	0.86 ± 0.30	↓ 1.7	0.00092
X75253	Phosphatidylethanolamine binding protein	1.37 ± 0.16	0.80 ± 0.15	↓ 1.7	<0.0001
Upregulated genes					
M81855	ATP-binding cassette, sub-family B (MDR/TAP), member 1 (P-glycoprotein/multidrug resistance 1)	0.02 ± 0.01	1.62 ± 0.50	↑ 80.2	<0.0001
AI169327	Tissue inhibitor of metalloproteinase 1	0.07 ± 0.04	2.65 ± 1.57	↑ 35.6	0.00014
M14656	Sialoprotein (osteopontin)	0.12 ± 0.04	4.19 ± 3.26	↑ 34.8	0.00121
AI169612	Adipocyte lipid-binding protein	0.07 ± 0.08	1.36 ± 0.50	↑ 19.1	<0.0001
J03627	S-100 related protein, clone 42C	0.16 ± 0.05	2.70 ± 1.86	↑ 17.2	0.00062
AI071531	Oxidized low density lipoprotein (lectin-like) receptor 1	0.22 ± 0.12	3.01 ± 1.52	↑ 13.9	<0.0001
X70871	Cyclin G1	0.20 ± 0.08	2.28 ± 0.81	↑ 11.6	<0.0001
AI639107	ESTs, similar to RIKEN cDNA C730007L20 gene (LOC364396), mRNA	0.14 ± 0.07	1.47 ± 0.43	↑ 10.2	<0.0001
AI639488	ESTs, highly similar to A42772 mdm2 protein-rat (*R. norvegicus*)	0.26 ± 0.05	2.59 ± 1.11	↑ 10.0	<0.0001
M58404	Thymosin, beta 10	0.18 ± 0.06	1.78 ± 0.88	↑ 9.6	<0.0001
M32062	Fc receptor, IgG, low affinity III	0.20 ± 0.07	1.90 ± 0.80	↑ 9.4	<0.0001
U49729	Bcl2-associated X protein	0.20 ± 0.10	1.90 ± 0.84	↑ 9.4	<0.0001
AI172064	Beta-galactoside-binding lectin	0.17 ± 0.06	1.61 ± 0.89	↑ 9.3	0.00016
AB010635	Carboxylesterase 2 (intestine, liver)	0.17 ± 0.05	1.49 ± 0.34	↑ 8.8	<0.0001
AA892506	Coronin, actin binding protein 1A	0.28 ± 0.16	2.49 ± 1.84	↑ 8.7	0.00164
AA819500	ESTs, highly similar to AC12_HUMAN ACTIVATOR 1 37 KD SUBUNIT (*H. sapiens*)	0.20 ± 0.19	1.77 ± 0.88	↑ 8.7	<0.0001
M63282	Activating transcription factor 3	0.37 ± 0.11	3.19 ± 2.43	↑ 8.6	0.00204
J02962	Lectin, galactose binding, soluble 3	0.18 ± 0.05	1.51 ± 0.49	↑ 8.4	<0.0001
M60921	B-cell translocation gene 2, anti-proliferative	0.30 ± 0.15	2.46 ± 1.95	↑ 8.3	0.00265
M35300	Serine protease inhibitor, kanzal type 1/trypsin inhibitor-like protein, pancreatic	0.40 ± 0.16	3.36 ± 1.06	↑ 8.3	<0.0001
X95986	Monomer; *R. norvegicus* CBR gene	0.22 ± 0.14	1.84 ± 0.88	↑ 8.3	<0.0001
AA892775	Lysozyme	0.17 ± 0.05	1.39 ± 0.33	↑ 8.2	<0.0001
X62952	Vimentin	0.19 ± 0.05	1.40 ± 0.35	↑ 7.4	<0.0001

TABLE 3
CONTINUED

GenBank Accession No.	Description	Mean ± SD of Control	Mean ± SD of DMN Treatment	Fold Change	*p*-Value
AA893246	ESTs, ATPase, H+ transporting, V1 subunit D	0.29 ± 0.06	1.79 ± 0.81	↑ 6.2	<0.0001
U18729	Cytochrome b558 alpha-subunit	0.23 ± 0.11	1.37 ± 0.79	↑ 6.0	0.00038
M57276	Leukocyte antigen (Ox-44)	0.30 ± 0.13	1.80 ± 0.56	↑ 5.9	<0.0001
AA859536	ESTs, brain abundant, membrane attached signal protein 1	0.32 ± 0.09	1.78 ± 0.81	↑ 5.5	<0.0001
AI233219	Pineal specific PG25 protein	0.38 ± 0.26	2.04 ± 0.79	↑ 5.4	<0.0001
X61654	CD63 antigen	0.30 ± 0.09	1.53 ± 0.76	↑ 5.2	0.00015
AI639029	ESTs, similar to lung inducible neuralized-related C3HC4 RING finger protein	0.45 ± 0.14	2.33 ± 1.36	↑ 5.2	0.00056
AI169104	ESTs, highly similar to PLATELET FACTOR 4 PRECURSOR (*R. norvegicus*)	0.35 ± 0.16	1.82 ± 0.97	↑ 5.1	0.00028
X62951	*Rattus norvegicus* mRNA (pBUS19) with repetitive elements	0.52 ± 0.19	2.61 ± 1.74	↑ 5.1	0.00151
AF001898	Aldehyde dehydrogenase 1, subfamily A1	0.24 ± 0.10	1.15 ± 0.47	↑ 4.8	<0.0001
U02320	*Rattus norvegicus* clone ndf40 neu differentiation factor mRNA, partial cds	0.42 ± 0.20	1.97 ± 0.58	↑ 4.7	<0.0001
J05122	Benzodiazepin receptor (peripheral)	0.44 ± 0.09	2.07 ± 1.01	↑ 4.7	0.00016
AA894004	ESTs, highly similar to CAPG MOUSE MACROPHAGE CAPPING PROTEIN (*M. musculus*)	0.41 ± 0.10	1.82 ± 0.90	↑ 4.5	0.00019
AI231821	Leukemia-associated cytosolic phosphoprotein stathmin	0.39 ± 0.10	1.71 ± 0.85	↑ 4.4	0.00021
AJ009698	Embigin	0.38 ± 0.14	1.55 ± 0.52	↑ 4.1	<0.0001
AA900505	rhoB gene	0.53 ± 0.12	2.09 ± 0.66	↑ 3.9	<0.0001
AF023087	NGFI-A; *Rattus norvegicus* nerve growth factor induced factor A mRNA, partial 3′UTR	0.35 ± 0.16	1.39 ± 0.38	↑ 3.9	<0.0001
AA891527	Four and a half LIM domains 2	0.33 ± 0.14	1.30 ± 0.38	↑ 3.9	<0.0001
X13044	CD74 antigen (invariant polpypeptide of major histocompatibility class II antigen-associated)	0.35 ± 0.10	1.36 ± 0.91	↑ 3.8	0.00271
X52196	Arachidonate 5-lipoxygenase activating protein	0.41 ± 0.08	1.53 ± 0.56	↑ 3.8	<0.0001
D13122	ATPase inhibitor (rat mitochondrial IF1 protein)	0.40 ± 0.09	1.48 ± 0.43	↑ 3.7	<0.0001
M76704	O^6-methylguanine-DNA methyltranferase	0.33 ± 0.07	1.20 ± 0.27	↑ 3.6	<0.0001
U25264	Selenoprotein W muscle 1	0.40 ± 0.16	1.44 ± 0.54	↑ 3.6	<0.0001
AI171966	*Rattus norvegicus* mRNA for RT1.Mb	0.37 ± 0.09	1.27 ± 0.49	↑ 3.5	<0.0001
X14254	Invariant chain (AA 1-280); rat mRNA for MHC class II-associated invariant chain	0.41 ± 0.10	1.39 ± 1.12	↑ 3.4	0.01136
AI008888	Cystatin beta	0.41 ± 0.12	1.36 ± 0.26	↑ 3.3	<0.0001
X13016	Rat mRNA for MRC OX-45 surface antigen	0.40 ± 0.11	1.32 ± 0.23	↑ 3.3	<0.0001
M12919	Aldolase A, fructose-bisphosphate	0.43 ± 0.10	1.41 ± 0.61	↑ 3.3	0.00015
U49930	Caspase 3, apoptosis related cysteine protease (ICE-like cysteine protease)	0.58 ± 0.11	1.91 ± 0.74	↑ 3.3	<0.0001
M83678	RAB13	0.48 ± 0.07	1.55 ± 0.78	↑ 3.3	0.00057
AF083269	Actin-related protein complex 1b	0.39 ± 0.08	1.26 ± 0.30	↑ 3.3	<0.0001
X52815	Cytoskeletal gamma-actin (AA 1-375); rat mRNA for cytoplasmic-gamma isoform of actin	0.45 ± 0.08	1.44 ± 0.40	↑ 3.2	<0.0001
U17919	Allograft inflammatory factor 1	0.37 ± 0.07	1.17 ± 0.38	↑ 3.2	<0.0001
AA799717	ESTs, polymerase (RNA) II (DNA directed) polypeptide I (predicted)	0.50 ± 0.13	1.57 ± 0.74	↑ 3.1	0.00039
AF017437	Integrin-associated protein	0.55 ± 0.18	1.71 ± 0.72	↑ 3.1	0.00014
X07944	Rat ornithine decarboxylase gene (EC 4.1.1.17)	0.57 ± 0.12	1.77 ± 0.76	↑ 3.1	0.00018
AA875523	ESTs, similar to myosin, light polypeptide 6, alkali, smooth muscle and non-muscle isoform 1 (*Canis familiaris*)	0.42 ± 0.11	1.30 ± 0.53	↑ 3.1	0.00011
M17412	Growth and transformation-dependent protein	0.55 ± 0.10	1.70 ± 0.83	↑ 3.1	0.00058
K02815	Butyrophilin-like 2 (MHC class II associated)	0.49 ± 0.20	1.47 ± 1.25	↑ 3.0	0.02078
AF065438	*Rattus norvegicus* mama mRNA, complete cds	0.43 ± 0.12	1.28 ± 0.48	↑ 3.0	<0.0001
AA892005	ESTs, SCIRP10-related protein	0.55 ± 0.10	1.59 ± 0.75	↑ 2.9	0.00058
J00797	Rat alpha-tubulin gene, exon 1	0.49 ± 0.16	1.42 ± 0.29	↑ 2.9	<0.0001
S57478	This sequence comes from Figure 2; lipocortin I (rats, genomic, 361 nt, segment 13 of 13)	0.44 ± 0.07	1.25 ± 0.41	↑ 2.9	<0.0001
X51707	Ribosomal protein S19 (AA 1-145); rat mRNA for ribosomal protein S19	0.47 ± 0.16	1.36 ± 0.47	↑ 2.9	<0.0001
M60666	Tropomyosin 1 (alpha)	0.54 ± 0.17	1.54 ± 0.36	↑ 2.8	<0.0001
D10587	*Rattus* sp. mRNA for 85kDa sialoglycoprotein (LGP85), complete cds	0.57 ± 0.20	1.61 ± 0.55	↑ 2.8	<0.0001

TABLE 3
CONTINUED

GenBank Accession No.	Description	Mean ± SD of Control	Mean ± SD of DMN Treatment	Fold Change	*p*-Value
U64030	dUTPase	0.47 ± 0.10	1.33 ± 0.27	↑ 2.8	<0.0001
M34253	Interferon regulatory factor 1	0.60 ± 0.17	1.64 ± 0.75	↑ 2.7	0.00051
X53517	CD37 antigen	0.51 ± 0.11	1.39 ± 0.72	↑ 2.7	0.00143
AI233173	Expressed in nonmetastatic cells 1, protein (NM23A) (nucleoside diphosphate kinase)	0.59 ± 0.08	1.58 ± 0.54	↑ 2.7	<0.0001
X78949	Prolyl 4-hydroxylase alpha subunit	0.56 ± 0.21	1.49 ± 0.40	↑ 2.6	<0.0001
X89225	*Rattus norvegicus* mRNA for protein linked to system L-like neutral amino acid transport activity	0.68 ± 0.33	1.77 ± 0.69	↑ 2.6	0.00017
M12156	Heterogeneous nuclear ribonucleoprotein A1	0.56 ± 0.10	1.42 ± 0.27	↑ 2.5	<0.0001
AF052596	Synaptosomal-associated protein, 23 kD	0.53 ± 0.18	1.34 ± 0.29	↑ 2.5	<0.0001
AB003042	Complement component 5, receptor 1	0.53 ± 0.13	1.32 ± 0.23	↑ 2.5	<0.0001
S72594	Tissue inhibitor of metalloproteinase type 2, TIMP-2	0.50 ± 0.06	1.24 ± 0.22	↑ 2.5	<0.0001
X05566	Rat mRNA for myosin regulatory light chain (RLC)	0.54 ± 0.10	1.35 ± 0.41	↑ 2.5	<0.0001
AF020618	Myeloid differentiation primary response gene 116	0.77 ± 0.12	1.91 ± 1.18	↑ 2.5	0.00667
X65228	*Rattus norvegicus* mRNA for ribosomal protein L23a	0.54 ± 0.20	1.33 ± 0.44	↑ 2.5	<0.0001
AA859305	*Rattus norvegicus* mRNA for tropomyosin isoform 6	0.52 ± 0.24	1.27 ± 0.31	↑ 2.4	<0.0001
AB015433	Solute carrier family 3 (activators of dibasic and neutral amino acid transport), member 2	0.69 ± 0.23	1.68 ± 0.63	↑ 2.4	0.00016
L19699	v-ral simian leukemia viral oncogene homolog B (ras related)	0.58 ± 0.08	1.40 ± 0.26	↑ 2.4	<0.0001
M15474	Striated-muscle alpha tropomyosin; Rat alpha-tropomyosin gene, exon 11	0.50 ± 0.18	1.21 ± 0.38	↑ 2.4	<0.0001
AA944397	ESTs, moderately similar to HS9B RAT HEAT SHOCK PROTEIN HSP 90-BETA (*R. norvegicus*)	0.52 ± 0.29	1.26 ± 0.44	↑ 2.4	0.00011
X54617	Rat RLC-A gene for myosin regulatory light chain, exon 4	0.52 ± 0.07	1.26 ± 0.26	↑ 2.4	<0.0001
AA892373	Syntenin	0.63 ± 0.11	1.51 ± 0.70	↑ 2.4	0.00117
D17445	Tyrosine 3-monooxygenase/tryptophan 5-monooxygenase activation protein, eta polypeptide	0.54 ± 0.15	1.30 ± 0.38	↑ 2.4	<0.0001
AA893670	ESTs, tumor protein D52 (predicted)	0.67 ± 0.16	1.61 ± 0.52	↑ 2.4	<0.0001
X78327	Ribosomal protein L13	0.59 ± 0.16	1.41 ± 0.52	↑ 2.4	0.00016
Y12635	ATPase, H+ transporting, lysosomal (vacuolar proton pump), beta 56/58 kDa, isoform 2	0.58 ± 0.18	1.36 ± 0.40	↑ 2.4	<0.0001
AI072634	*Rattus norvegicus* cytokeratin-18 mRNA, partial cds	0.71 ± 0.22	1.68 ± 0.53	↑ 2.4	<0.0001
L03201	Cathepsin S	0.46 ± 0.15	1.07 ± 0.36	↑ 2.3	<0.0001
AA860030	*Rattus norvegicus* mRNA for class I beta-tubulin, complete cds	0.58 ± 0.06	1.36 ± 0.46	↑ 2.3	0.00010
M63983	Hypoxanthine guanine phosphoribosyl transferase	0.53 ± 0.13	1.24 ± 0.30	↑ 2.3	<0.0001
U60882	Heterogeneous nuclear ribonucleoproteins methyltransferase-like 2 (*S. cerevisiae*)	0.61 ± 0.20	1.41 ± 0.44	↑ 2.3	<0.0001
J02780	Tropomyosin 4	0.54 ± 0.11	1.26 ± 0.19	↑ 2.3	<0.0001
M31038	RT1 class Ib gene	0.64 ± 0.33	1.48 ± 0.61	↑ 2.3	0.00068
AA944856	RAP1B, member of RAS oncogene family	0.63 ± 0.12	1.44 ± 0.23	↑ 2.3	<0.0001
X76453	HRAS like suppressor	0.58 ± 0.27	1.32 ± 0.45	↑ 2.3	0.00011
AA892851	ESTs, protein tyrosine kinase 9 (predicted)	0.61 ± 0.28	1.38 ± 0.69	↑ 2.3	0.00271
AA892308	ESTs, similar to hypothetical protein D11Ertd497e (predicted)	0.66 ± 0.12	1.50 ± 0.53	↑ 2.3	0.00018
AA893584	ESTs, biogenesis of lysosome-related organelles complex-1, subunit 2 (predicted)	0.65 ± 0.20	1.47 ± 0.50	↑ 2.2	0.00012
AI009806	Dynein, cytoplasmic, light chain 1	0.56 ± 0.08	1.26 ± 0.18	↑ 2.2	<0.0001
S82383	TM-5; slow-twitch alpha TM/hTMnm homolog (rats, macrophages, mRNA partial, 1742 nt)	0.52 ± 0.10	1.16 ± 0.21	↑ 2.2	<0.0001
U21871	*Rattus norvegicus* outer mitochondrial membrane receptor rTOM20 mRNA, complete cds	0.69 ± 0.20	1.52 ± 0.48	↑ 2.2	<0.0001
M37584	H2A histone family, member Z	0.57 ± 0.19	1.26 ± 0.32	↑ 2.2	<0.0001
AI235585	Cathepsin D	0.61 ± 0.24	1.33 ± 0.33	↑ 2.2	<0.0001
AI228738	FK506-binding protein 1 (12kD)	0.61 ± 0.13	1.32 ± 0.40	↑ 2.2	<0.0001
AA899253	Myristoylated alanine-rich protein kinase C substrate	0.56 ± 0.13	1.18 ± 0.36	↑ 2.1	<0.0001
D42116	*Rattus norvegicus* mRNA for 5I2 antigen, clone 17, partial cds	0.55 ± 0.11	1.15 ± 0.23	↑ 2.1	<0.0001
AI177096	ESTs, highly similar to APT RAT ADENINE PHOSPHORIBOSYLTRANSFERASE (*R. norvegicus*)	0.65 ± 0.09	1.36 ± 0.32	↑ 2.1	<0.0001
D84477	*Rattus norvegicus* mRNA for RhoA, partial cds	0.58 ± 0.21	1.20 ± 0.23	↑ 2.1	<0.0001
M12672	GTP-binding protein (G-alpha-i2)	0.58 ± 0.12	1.21 ± 0.28	↑ 2.1	<0.0001
AI169417	Phosphoglycerate mutase 1	0.70 ± 0.21	1.43 ± 0.44	↑ 2.0	0.00011

TABLE 3
CONTINUED

GenBank Accession No.	Description	Mean ± SD of Control	Mean ± SD of DMN Treatment	Fold Change	*p*-Value
X78167	*Rattus norvegicus* (Sprague Dawley) ribosomal protein L15 mRNA	0.64 ± 0.12	1.29 ± 0.30	↑ 2.0	<0.0001
AI231292	Cystatin C (cysteine proteinase inhibitor)	0.58 ± 0.15	1.17 ± 0.28	↑ 2.0	<0.0001
AF052042	*Rattus norvegicus* zinc finger protein Y1 (RLZF-Y) mRNA, complete cds	0.61 ± 0.22	1.22 ± 0.28	↑ 2.0	<0.0001
AA799545	ESTs, weakly similar to TCPA RAT T-COMPLEX PROTEIN 1, ALPHA SUBUNIT (*R. norvegicus*)	0.74 ± 0.21	1.46 ± 0.46	↑ 2.0	0.00017
AA892014	HLA-B associated transcript 1A	0.73 ± 0.20	1.44 ± 0.36	↑ 2.0	<0.0001
X58465	Rat mRNA for ribosomal protein S5	0.64 ± 0.11	1.28 ± 0.22	↑ 2.0	<0.0001
AA799501	NADH ubiquinone oxidoreductase subunit B13	0.72 ± 0.19	1.42 ± 0.40	↑ 2.0	<0.0001
AI169370	Alpha-tubulin	0.60 ± 0.14	1.19 ± 0.18	↑ 2.0	<0.0001
AF022083	Guanine nucleotide-binding protein beta 1	0.71 ± 0.15	1.40 ± 0.29	↑ 2.0	<0.0001
U44948	Cysteine-rich protein 2	0.75 ± 0.14	1.47 ± 0.21	↑ 2.0	<0.0001
AA942751	Tyrosine 3-monooxygenase/tryptophan 5-monooxygenase activation protein, theta polypeptide	0.65 ± 0.15	1.25 ± 0.23	↑ 1.9	<0.0001
X62322	Granulin	0.57 ± 0.23	1.08 ± 0.31	↑ 1.9	0.00020
X02904	Glutathione *S*-transferase, pi 2	0.67 ± 0.15	1.27 ± 0.33	↑ 1.9	<0.0001
AI639132	ESTs, similar to RIKEN cDNA 6720467C03 (predicted)	0.76 ± 0.16	1.41 ± 0.28	↑ 1.9	<0.0001
L38615	Glutathione synthetase gene	0.63 ± 0.13	1.15 ± 0.15	↑ 1.8	<0.0001
U13895	*Rattus norvegicus* MSS1 protein (MSS1) mRNA, partial cds	0.73 ± 0.22	1.33 ± 0.25	↑ 1.8	<0.0001
X14181	Ribosomal protein L18a (AA 1-175); rat mRNA for ribosomal protein L18a	0.72 ± 0.15	1.27 ± 0.27	↑ 1.8	<0.0001
AA944324	ADP-ribosylation factor 6	0.69 ± 0.10	1.19 ± 0.14	↑ 1.7	<0.0001
AI178135	Complement component 1, q subcomponent binding protein	0.77 ± 0.18	1.26 ± 0.15	↑ 1.6	<0.0001

Genes are ranked by fold change.
Significance was calculated using the *t*-test.

tion (I0–I3) scores, fibrosis (F0–F3), and fatty change (classified as presence or absence; +/–). In the first 2 weeks, bridging (N2, 50%) and hemorrhagic confluent necrosis (N3, 50%) were found in all rats treated with DMN. By the third to fourth week, hemorrhagic confluent necrosis (N3) was found in most DMN-treated rats (91%). In the last 2 weeks, necrosis disappeared or regressed to a low level in small regions (N1, 12.5%). In addition, our data also suggest that the 3-week treatment with a low dose of DMN induced diffuse bridging necrosis without steatosis in this rat model system. Similarly, the majority of the DMN-treated rats displayed high inflammatory infiltration, ranging from moderate (I2, 50%) to marked (I3, 50%), during the first 2 weeks. By the third to fourth week, the intensity of inflammatory cell infiltration at portal areas was still high in most DMN-treated rats (I2, 54.5% and I3, 27.2%). In the last 2 weeks, a significant regression of liver damage to a low level in small regions (I0, 75% and I1, 12.5%) was observed. Together, for the combined necrosis and inflammation scores, mild (A1–3, 62.5%) and moderate necroinflammatory (A4–6, 36.5%) patterns were found in all rats treated with DMN in the first 2 weeks (Fig. 5B). By the third to fourth week, hemorrhagic confluent necrosis, combined with portal inflammation, was found in most DMN-treated rats (A4–6, 64%). However, in the fifth to sixth week, both necrosis and inflammation had disappeared (A0, 44%) or had regressed to a low level (A1–3, 44%) in small regions.

Seventy-five percent of the DMN-treated rats had none (F0) or low levels of fibrosis (F1) in the first 2 weeks. By the third to fourth week, nearly 90% of the DMN-treated rats had high levels of fibrosis, from bridging fibrosis (F2) to frequent bridging fibrosis with focal nodule formation (F3). In the last 2 weeks, F2 and F3 were still present in 78% of DMN-treated rats. The fatty changes were only present in a few treated rats (3.7%). In contrast, there were no abnormal pathological patterns present in the control group at all (Fig. 5B). In addition, no clear abnormality was found in the kidney or spleen of the DMN-treated and normal rats (data not shown). All of the histopathological datasets have been deposited on our liver fibrosis website (see below). Together, the detailed necroinflammatory and fibrosis scoring systems of the process of the DMN-induced liver damage suggest that dramatic necrosis and inflammation took place during early liver damage progression

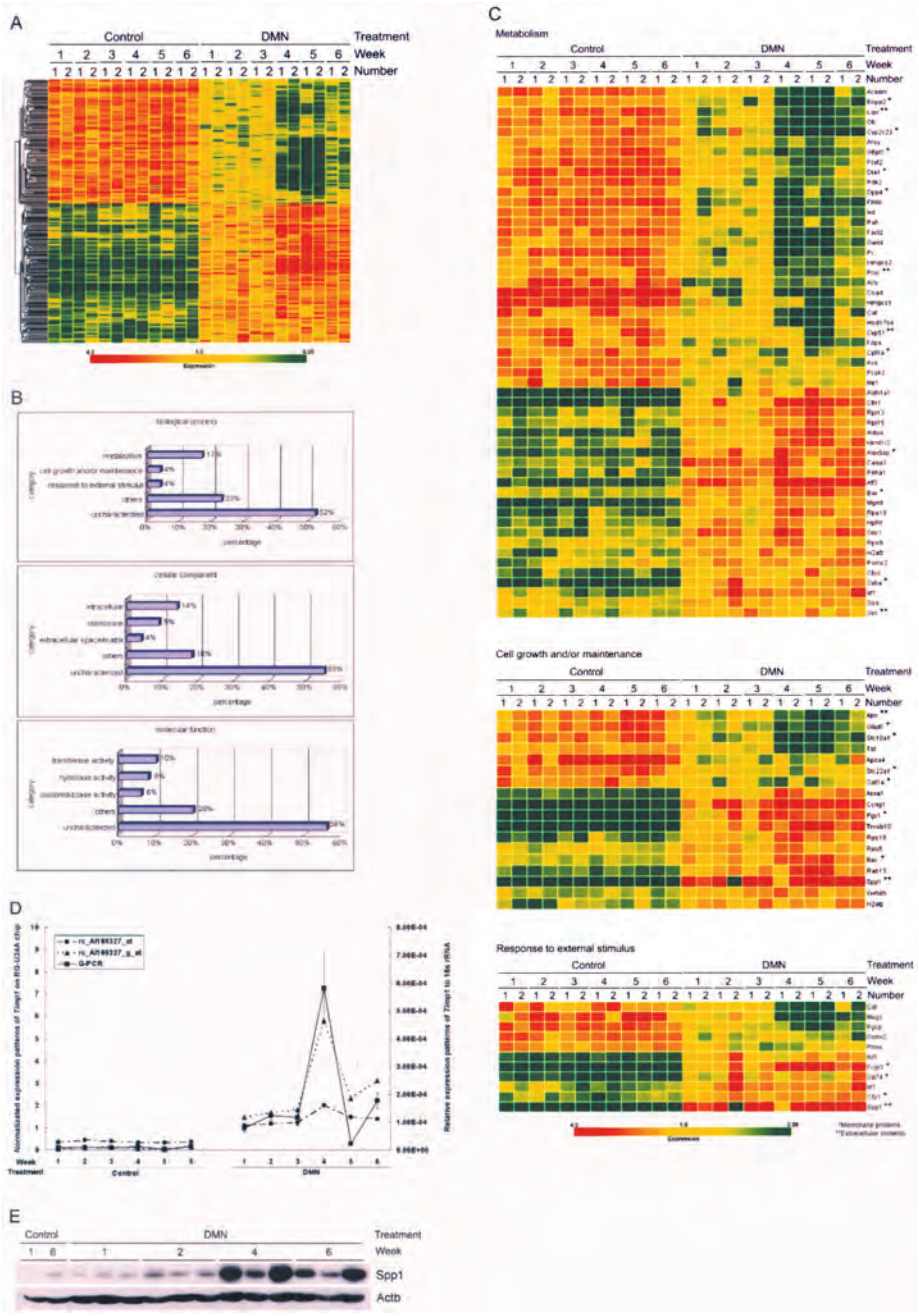

Figure 4. The 256 gene expression patterns of experimental samples. (A) Hierarchical clustering results of these gene expression patterns. The results are shown in a diagram format, in which rows represent individual transcripts and columns represent time course sample. The color in each cell reflected the expression level of the corresponding sample, relative to its mean expression level. The scale extends from fluorescence ratios of 0.25 to 4 relative to the mean level for all samples. (B) Gene ontology results of 256 genes. The plots of different category of these genes by gene ontology database (http://fatigo.bioinfo.cnif.es/). (C) The hierarchical clustering results of the three biology processes are: metabolism, cell growth and/or maintenance and response stimulus. These diagrams are formatted as rows representing individual transcripts and columns representing time course sample. The color in each cell reflects the expression level of the corresponding sample relative to its mean expression level and the scale extends from fluorescence ratios of 0.25 to 4 relative to the mean level for all samples. (D) The comparison of *Timp1* expression between the Q-RT-PCR results and microarray data. The TaqMan® assays were conducted in triplicate for each sample, and a mean value was used for calculation of expression levels (marked by the square). To standardize the quantification of the *Timp1*, 18S rRNA from each sample was quantified at the same time as the target gene and a log scale was used as indicated on the right side of plot. For the two *Timp1* transcripts, rc_AI169327_at and rc_AI169327_g_at (marked by circle and triangle), the expression levels of the microarray data were relative to the mean of all gene expression levels and the scale is indicated on the left side of plot. The Pearson correlation coefficients (*r*), which compared the Q-RT-PCR result and the microarray data of two *Timp1* transcripts (rc_AI169327_at and rc_AI169327_g_at), were 0.79 and 0.92, respectively. (E) Endogenous Spp1 protein expression pattern in DMN-induced rat liver samples. Rat liver samples were lysed and 50 μg protein lysates were subjected to immunoblot analysis with antibody against Spp1 and Actb. Spp1 was significantly overexpressed at the protein level after the fourth week of DMN treatment.

A

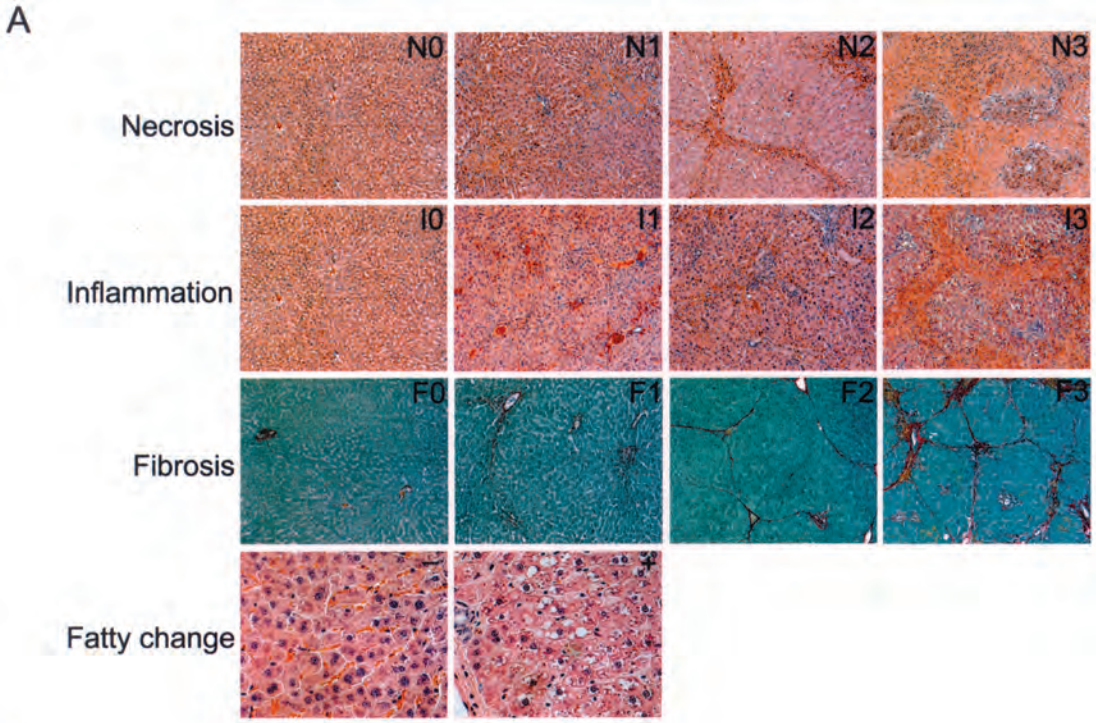

B

Factor (scores)		DMN-treatment 1-2 wk n (%)	DMN-treatment 3-4 wk n (%)	DMN-treatment 5-6 wk n (%)	Control 1-6 wk n (%)
Necroinflammatory	A0	0 (0)	1 (9)	4 (44)	100 (24)
	A(1-3)	5 (62.5)	3 (27)	4 (44)	0 (0)
	A(4-6)	3 (36.5)	7 (64)	1 (12)	0 (0)
Fibrosis	F(0-1)	6 (75)	1 (9)	2 (22)	100 (24)
	F(2-3)	2 (25)	10 (91)	7 (78)	0 (0)
Fatty change	-	7 (87.5)	11 (100)	9 (100)	100 (24)
	+	1 (12.5)	0 (0)	0 (0)	0 (0)

n: number of rats

Figure 5. Histopathological analysis reveals DMN-induced rat liver damage. (A) The representative phenotype of the DMN-induced rat liver fibrosis was characterized by scoring the four histopathological features as follows: the necrosis scores were from N0 to N3 (the first panel), the inflammation scores were from I0 to I3 (the second panel), the fibrosis scores were from F0 to F3 (the third panel), and the fatty change scores were presence or absence (+ and −) (the last panel). The necroinflammatory scores were the sum of the necrosis and inflammation scores and range from A0 to A6. The images of the fatty change are shown at 200× original magnification, whereas the others are shown at 100× original magnification. (B) The summary of histopathological scores for the rat model. The results were ranked by time course. Necroinflammatory change was divided into three grades: A0 = "no," A(1–3) = "mild," and A(4–6) = "moderate" necroinflammation. Fibrosis is divided into two grades: F(0–1) = "normal to fibrous expansion of portal tracts" and F(2–3) = "bridge fibrosis to frequent bridging fibrosis with nodule formation." The fatty change is shown as presence or absence (+/–). The number of rats was counted and used to calculate the percentage of each histopathological level at each time point.

(weeks 1–4) and this was followed by hepatic bridging fibrosis at 3–6 weeks.

Necroinflammatory and Fibrosis Candidate Genes

Necroinflammatory and fibrosis have been suggested to play important roles in liver cirrhosis progression in the rat model (1,13,24,25,27). To clarify the factors responsible for this histopathological phenotype, all rat samples were classified by histopathological evaluation with histopathological scores for necroinflammatory (A0–A6) and fibrosis (F0–F3) as describe in Figure 5B. Comparing mRNA expression levels from microarray data, 44 genes were identified by expression level to be significantly correlated with none to higher scores by the LSM method at the 5% significance level, which was separately estimated for each three-subgroup variation in necroinflammatory score (Fig. 6A and Table 4). Of these 44 genes, 33 of them were expressed at higher levels in liver with necroinflammation compared to the normal liver and of these nine were membrane or extracellular proteins as annotated by gene ontology (Fig. 6A). These nine genes might have potential to serve as marker signatures for necroinflammation. Among these 44 genes, the results for two of them [endothelial cell-specific molecule 1 (*Esm1*) and vimentin (*Vim*)] are consistent with previous studies that examined individual markers (see the Discussion) (6,38).

Using the Student's *t*-test, 62 differentially expressed genes (32 upregulated and 30 downregulated) between the F0–1 and F2–3 level of fibrosis were identified at the 5% significance level, estimated using only two subgroup variations for the fibrosis score (Fig. 6C, and Table 5). Similarly, annotation based on the gene ontology database revealed that there were 15 membrane and extracellular proteins that showed a fibrosis signature. In agreement with previous studies, three genes, including *Timp1*, *CD63*, antigen (*Cd63*), and annexin A1 (*Anxa1*), exhibited similar gene expression patterns during liver fibrosis (3,22,32,43). These necroinflammatory and fibrosis-associated gene expression patterns were plotted over the time course (Fig. 6B, 6D). The color corresponds to relative gene expression using the first week as the control. These observations indicated that oligo-microarray analysis is a powerful approach for monitoring molecular events during liver injury and repair where the pathogenesis is unknown, and these signature genes could discriminate successfully between the low-score and the high-score histopathology groups. Together, the genes would seem to be responsible for the early stage formation of necroinflammation and fibrosis; thus, we believe they are possible early markers for the detection of fibrosis.

Data Comparison

To assess the validity of our expression cassette of genes for distinguishing liver damage from rat liver sample specimens, we explored the overlap between our data and other published studies. We compared with four datasets. First was the intersection between our 256 significant genes and the Utsunomiya et al. gene lists, which identified 100 differentially expressed genes in TAA-induced liver fibrosis using rat cDNA microarray (45). Of these 100 genes, 14 genes, including 7 genes upregulated and 7 genes downregulated, overlapped with th our most significant 256 gene list as shown in Table 6. Failure to detect the remaining genes is probably due to most of them having "absent" calls in Affymetrix chips. Therefore, these genes did not qualify under the conditions of our analysis. Alternatively, TAA and DMN might induce different responses during liver fibrosis. In addition, there can be substantial variation in the data, which can be generated across multiple microarray platforms during the course of data analysis. Therefore, it is not surprising that only a few genes overlapped in this data comparison (44). Secondly, to allow a comparison against microarray data from patients with cirrhosis (26), we converted the most significant 256 rat genes by the GeneSpring software homology table and the HomoloGene NCBI database (http://www.ncbi.nlm.nih.gov/entrez/query.fcgi?db=homologene) into their human ortholog genes, and 213 genes were listed. From studies by Kim and his colleagues, the results showed that 8 genes, including 6 genes in the hepatocellular carcinoma-associated signature table and 2 genes in etiology-associated signature table overlapped with our most significant human homolog gene list (26) (Table 6). Even though only a few genes overlapped in this data comparison, these 213 gene expression pattern changes might aid for the detection of human early liver injury. Thirdly, the liver sample response to injury includes both hepatic bridging fibrosis and regeneration with the outcome determined by the injury (46). On comparing White's study (50) with our 256 genes, there were 21 upregulated and 13 downregulated genes that occurred in both datasets. These overlapping genes might be referred to as liver regeneration signatures. Finally, 14 out of 39 well-known fibrosis markers (13,19,23) could be found in our results (Supplemental Table 1). Two, including *Timp1* and *Timp2*, out of 14 genes share similar gene expression patterns to the human liver damage phenotype against our microarray dataset, as shown in Supplemental Table 2. The results suggest that these findings from a study generated using an animal model system should be extendable to clinical studies. When the liver is sub-

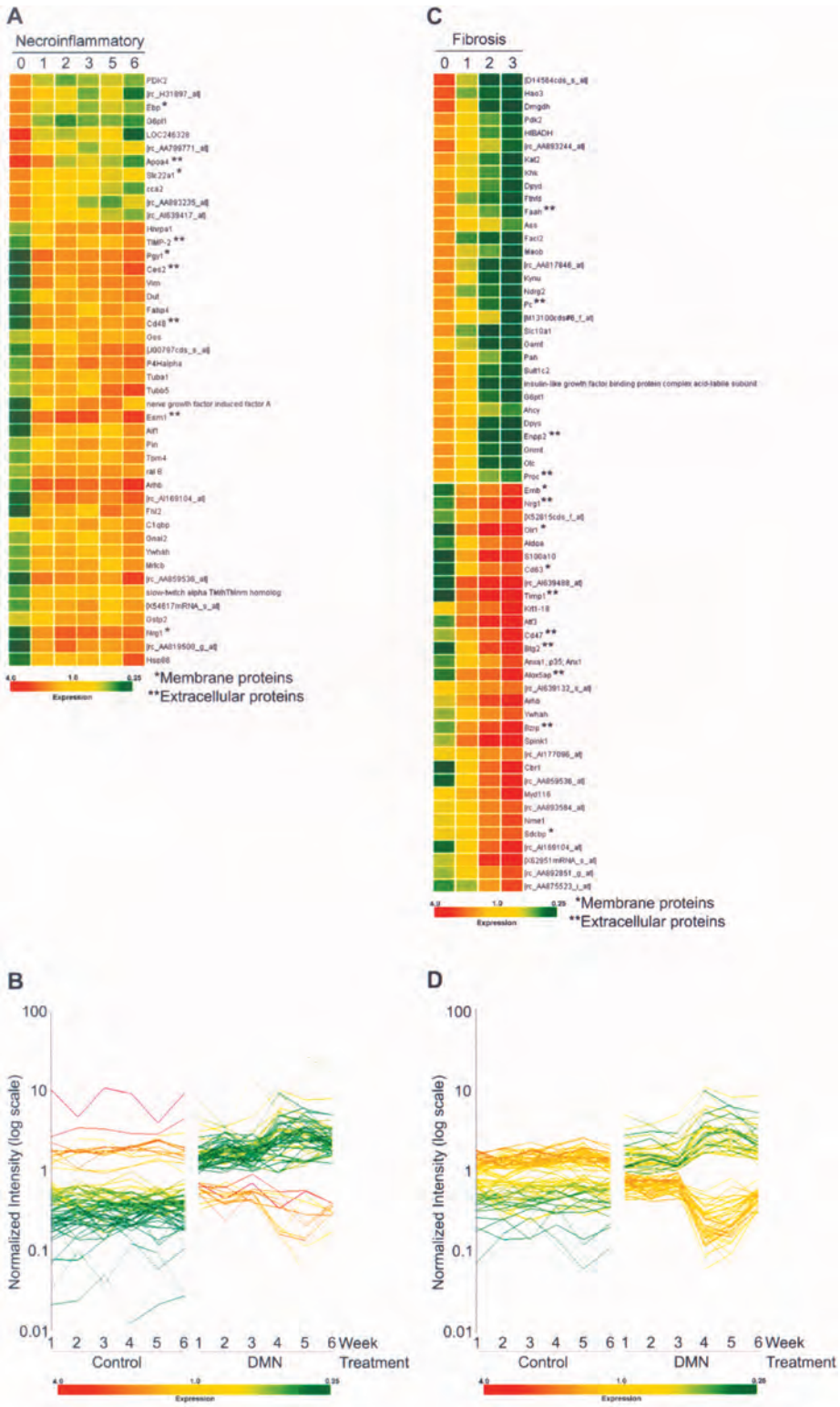

Figure 6. The associated genes related to necroinflammatory and fibrosis progression. The genes related to the necroinflammatory (A) and fibrosis scores (C) were filtered from the 256 genes by their different fibrosis levels. Both upregulated and downregulated expression patterns of the necroinflammatory or fibrosis-related genes were compared against the patterns at score A0 or F0. Altogether 44 genes (35 genes and 9 ESTs) were found to be related to necroinflammatory and 62 genes (48 genes and 14 ESTs) were found to be related to the fibrosis process. Both the necroinflammatory and fibrosis-associated gene expression patterns were plotted against a time course (B and D). The color corresponds to the relative gene expression at the control first week. The scale extends from fluorescence radios of 0.25 to 4 relative to the mean level for all samples.

TABLE 4
GENES WITH MOST SIGNIFICANT CHANGES IN EXPRESSION BETWEEN LOW AND HIGH SCORES OF NECROINFLAMMATION

GenBank Accession No.	Description	Mean ± SD of Necroinflammatory Scores 0	1–3	4–6	*p*-Value
Downregulated genes					
U10357	Pyruvate dehydrogenase kinase 2	1.70 ± 0.34	0.63 ± 0.20	0.64 ± 0.14	<0.0001
AA893235	ESTs, moderate similarity to protein sp:P27469 (*H. sapiens*) G0S2_HUMAN putative lymphocyte G0/G1 switch protein 2	1.78 ± 0.72	0.80 ± 0.41	0.60 ± 0.09	0.001
AA799771	ESTs, EST189268 normalized rat heart, Bento Soares *Rattus* sp. cDNA clone RHEAF15 3-end, mRNA sequence	1.78 ± 0.47	0.75 ± 0.25	0.75 ± 0.15	<0.0001
H31897	ESTs, EST106437 Rat PC-12 cells, untreated *Rattus norvegicus* cDNA clone RPCBC56 3-end, mRNA sequence	1.48 ± 0.32	0.71 ± 0.29	0.64 ± 0.23	<0.0001
AF080468	Glucose-6-phosphatase, transport protein 1	1.62 ± 0.45	0.58 ± 0.30	0.56 ± 0.04	<0.0001
AA893552	Kallistatin	2.70 ± 0.52	0.65 ± 0.28	0.66 ± 0.27	<0.0001
M00002	Apolipoprotein A-IV	2.99 ± 1.34	0.80 ± 0.34	0.60 ± 0.17	<0.0001
H33491	Phenylalkylamine Ca^{2+} antagonist (emopamil) binding protein	1.67 ± 0.44	0.65 ± 0.20	0.67 ± 0.21	<0.0001
X78855	Solute carrier family 22, member 1	1.58 ± 0.38	0.85 ± 0.19	0.74 ± 0.06	<0.0001
AI639417	ESTs, membrane targeting (tandem) C2 domain containing 1	1.50 ± 0.47	0.93 ± 0.29	0.66 ± 0.23	0.002
AB000199	CCA2 protein	1.50 ± 0.48	0.81 ± 0.23	0.65 ± 0.28	0.0006
Upregulated genes					
M12156	Heterogeneous nuclear ribonucleoprotein A1	0.56 ± 0.10	1.35 ± 0.29	1.60 ± 0.09	<0.0001
U64030	Deoxyuridinetriphosphatase (dUTPase)	0.47 ± 0.10	1.28 ± 0.24	1.46 ± 0.40	<0.0001
L38615	Glutathione synthetase	0.63 ± 0.13	1.14 ± 0.18	1.18 ± 0.07	<0.0001
AI169370	ESTs, *Rattus norvegicus* similar to tubulin alpha-1 chain—Chinese hamster (LOC300217), mRNA	0.60 ± 0.14	1.13 ± 0.17	1.37 ± 0.06	<0.0001
AI009806	Dynein, cytoplasmic, light chain 1	0.56 ± 0.08	1.26 ± 0.20	1.23 ± 0.14	<0.0001
M12672	GTP-binding protein (G-alpha-i2)	0.58 ± 0.12	1.17 ± 0.31	1.31 ± 0.20	<0.0001
S72594	Tissue inhibitor of metalloproteinase type 2, TIMP-2T	0.50 ± 0.06	1.24 ± 0.24	1.23 ± 0.20	<0.0001
AB010635	Carboxylesterase 2 (intestine, liver)	0.17 ± 0.05	1.41 ± 0.29	1.73 ± 0.42	<0.0001
J02780	Tropomyosin 4	0.54 ± 0.11	1.24 ± 0.19	1.29 ± 0.24	<0.0001
AI169104	ESTs, weak similarity to protein sp:P02776 (*H. sapiens*) PLF4_HUMAN Platelet factor 4 precursor (PF-4)	0.35 ± 0.16	1.86 ± 1.12	1.70 ± 0.45	0.0002
AA944397	Heat shock protein 86	0.52 ± 0.29	1.19 ± 0.37	1.47 ± 0.64	0.0003
D17445	Tyrosine 3-monooxygenase/tryptophan 5-monooxygenase activation protein, eta polypeptide	0.54 ± 0.15	1.30 ± 0.44	1.29 ± 0.18	<0.0001
J00797	Rat alpha-tubulin gene, exon 1	0.49 ± 0.16	1.31 ± 0.25	1.74 ± 0.11	<0.0001
U02320	Neuregulin 1	0.42 ± 0.20	2.02 ± 0.68	1.81 ± 0.07	<0.0001
AA900505	rhoB gene	0.53 ± 0.12	2.10 ± 0.72	2.07 ± 0.55	<0.0001
AA891527	Four and a half LIM domains 2	0.33 ± 0.14	1.18 ± 0.34	1.65 ± 0.30	<0.0001
X62952	Vimentin	0.19 ± 0.05	1.34 ± 0.36	1.57 ± 0.27	<0.0001
X78949	Prolyl 4-hydroxylase alpha subunit	0.56 ± 0.21	1.44 ± 0.44	1.65 ± 0.25	<0.0001
M81855	P-glycoprotein/multidrug resistance 1	0.03 ± 0.01	1.59 ± 0.50	1.71 ± 0.56	<0.0001
AA860030	Tubulin, beta 5	0.58 ± 0.06	1.16 ± 0.29	1.96 ± 0.33	<0.0001
X05566	Myosin regulatory light chain	0.54 ± 0.10	1.41 ± 0.45	1.17 ± 0.20	<0.0001
X02904	Glutathione *S*-transferase, pi 2	0.67 ± 0.15	1.30 ± 0.35	1.17 ± 0.27	<0.0001
X13016	CD48 antigen	0.40 ± 0.11	1.31 ± 0.22	1.35 ± 0.28	<0.0001
S82383	TM-5; slow-twitch alpha TM/hTMnm homolog (rats, macrophages, mRNA partial, 1742 nt)	0.52 ± 0.10	1.18 ± 0.24	1.09 ± 0.13	<0.0001
AI233219	Endothelial cell-specific molecule 1	0.38 ± 0.26	2.14 ± 0.85	1.75 ± 0.65	<0.0001
AA859536	ESTs, brain abundant, membrane attached signal protein 1	0.32 ± 0.09	1.82 ± 0.87	1.65 ± 0.69	<0.0001
AI178135	Complement component 1, q subcomponent binding protein	0.77 ± 0.18	1.26 ± 0.15	1.24 ± 0.18	<0.0001
AA819500	ESTs, moderate similarity to protein ref:NP_002907.1 (*H. sapiens*) replication factor C (activator 1) 4 (37 kD)	0.20 ± 0.19	1.90 ± 0.98	1.41 ± 0.41	<0.0001
AI169612	Fatty acid binding protein 4	0.07 ± 0.08	1.36 ± 0.56	1.38 ± 0.34	<0.0001
L19699	v-ral simian leukemia viral oncogene homolog B	0.58 ± 0.08	1.42 ± 0.30	1.36 ± 0.01	<0.0001
U17919	Allograft inflammatory factor 1	0.37 ± 0.07	1.17 ± 0.43	1.16 ± 0.26	<0.0001
AF023087	Early growth response 1	0.35 ± 0.16	1.34 ± 0.33	1.55 ± 0.55	<0.0001
X54617	Rat RLC-A gene for myosin regulatory light chain, exon 4	0.52 ± 0.07	1.30 ± 0.27	1.11 ± 0.19	<0.0001

Significance was calculated using least squares means of ANOVA.

TABLE 5
GENES WITH MOST SIGNIFICANT CHANGES IN EXPRESSION BETWEEN LOW AND HIGH SCORES OF FIBROSIS

GenBank Accession No.	Description	Mean ± SD of Fibrosis Score 0–1	Mean ± SD of Fibrosis Score 2–3	Fold Change	*p*-Value
Downregulated genes					
D14564	*Rattus norvegicus* gene for L-gulono-gamma-lactone oxidase, exon 7	2.48 ± 1.21	0.38 ± 0.28	↓ 6.6	<0.0001
AA892345	Dimethylglycine dehydrogenase precursor	2.23 ± 1.07	0.42 ± 0.27	↓ 5.3	<0.0001
AI232087	*Rattus norvegicus* transcribed sequences	2.05 ± 0.83	0.49 ± 0.28	↓ 4.2	<0.0001
M77479	Solute carrier family 10, member 1	1.42 ± 0.58	0.36 ± 0.33	↓ 4.0	<0.0001
S46785	Insulin-like growth factor binding protein complex acid-labile subunit (rats, liver, mRNA, 2190 nt)	1.69 ± 0.59	0.47 ± 0.29	↓ 3.6	<0.0001
U68168	Kynureninase (L-kynurenine hydrolase)	1.61 ± 0.58	0.47 ± 0.35	↓ 3.4	<0.0001
U32314	Pyruvate carboxylase	1.59 ± 0.63	0.48 ± 0.33	↓ 3.3	<0.0001
D90109	Fatty acid Coenzyme A ligase, long chain 2	1.42 ± 0.52	0.44 ± 0.26	↓ 3.3	<0.0001
D28560	Ectonucleotide pyrophosphatase/phosphodiesterase 2	1.27 ± 0.40	0.39 ± 0.34	↓ 3.2	<0.0001
AF080468	Glucose-6-phosphatase, transport protein 1	1.42 ± 0.53	0.45 ± 0.16	↓ 3.2	<0.0001
AA817846	ESTs, strong similarity to protein ref:NP_004042.1 (*H. sapiens*) 3-hydroxybutyrate dehydrogenase precursor	1.43 ± 0.52	0.45 ± 0.40	↓ 3.2	<0.0001
AA926193	Sulfotransferase family, cytosolic, 1C, member 2	1.56 ± 0.57	0.50 ± 0.28	↓ 3.1	<0.0001
X06150	Glycine methyltransferase	1.45 ± 0.45	0.48 ± 0.34	↓ 3.0	<0.0001
M59861	10-Formyltetrahydrofolate dehydrogenase	1.54 ± 0.66	0.52 ± 0.33	↓ 3.0	<0.0001
D63704	Dihydropyrimidinase	1.42 ± 0.32	0.48 ± 0.29	↓ 3.0	<0.0001
M11266	Ornithine transcarbamylase	1.35 ± 0.42	0.46 ± 0.26	↓ 2.9	<0.0001
AA799560	N-myc downstream-regulated gene 2	1.35 ± 0.43	0.48 ± 0.30	↓ 2.8	<0.0001
AA893244	ESTs, moderate similarity to protein pdb:1LBG (*E. coli*) B Chain B	1.88 ± 0.74	0.67 ± 0.24	↓ 2.8	<0.0001
D85035	Dihydropyrimidine dehydrogenase	1.43 ± 0.44	0.53 ± 0.21	↓ 2.7	<0.0001
U10357	Pyruvate dehydrogenase kinase 2	1.48 ± 0.49	0.55 ± 0.14	↓ 2.7	<0.0001
J03588	Guanidinoacetate methyltransferase	1.12 ± 0.34	0.41 ± 0.30	↓ 2.7	<0.0001
U72497	Fatty acid amide hydrolase	1.56 ± 0.57	0.58 ± 0.25	↓ 2.7	<0.0001
Z50144	Kynurenine aminotransferase 2	1.37 ± 0.36	0.53 ± 0.34	↓ 2.6	<0.0001
M23601	Monoamine oxidase B	1.45 ± 0.44	0.60 ± 0.37	↓ 2.4	0.0001
M12337	Phenylalanine hydroxylase	1.39 ± 0.35	0.61 ± 0.20	↓ 2.3	<0.0001
AI013861	3-Hydroxyisobutyrate dehydrogenase	1.27 ± 0.37	0.56 ± 0.22	↓ 2.3	<0.0001
M86235	*Rattus norvegicus* mRNA for ketohexokinase	1.19 ± 0.32	0.54 ± 0.18	↓ 2.2	<0.0001
X64336	Protein C	1.23 ± 0.40	0.59 ± 0.20	↓ 2.1	<0.0001
M15185	*S*-Adenosyl-L-homocysteine hydrolase (EC 3.3.1.1); rat *S*-adenosyl-L-homocysteine hydrolase mRNA, complete cds	1.28 ± 0.34	0.63 ± 0.14	↓ 2.0	<0.0001
X12459	Arginosuccinate synthetase	1.40 ± 0.38	0.73 ± 0.20	↓ 1.9	<0.0001
M13100	ORFa′; ORFa; ORFb; ORFc; ORFd1; ORFd2; putative; rat long interspersed repetitive DNA sequence LINE3 (L1Rn)	1.32 ± 0.59	0.69 ± 0.29	↓ 1.9	0.0022
Upregulated genes					
AI169327	Tissue inhibitor of metalloproteinase 1	0.43 ± 0.65	3.23 ± 1.65	↑ 7.4	0.0017
J03627	S-100 related protein, clone 42C	0.46 ± 0.55	3.37 ± 1.98	↑ 7.3	0.0041
AI071531	Oxidized low density lipoprotein (lectin-like) receptor 1	0.56 ± 0.62	3.73 ± 1.36	↑ 6.7	0.0002
M60921	B-cell translocation gene 2, anti-proliferative	0.56 ± 0.50	3.03 ± 2.20	↑ 5.4	0.0154
M63282	Activating transcription factor 3	0.77 ± 0.74	3.80 ± 2.82	↑ 4.9	0.0189
X95986	Monomer; *Rattus norvegicus* CBR gene	0.48 ± 0.54	2.14 ± 0.88	↑ 4.5	0.0007
AA859536	*Rattus norvegicus* transcribed sequences	0.49 ± 0.32	2.16 ± 0.72	↑ 4.4	0.0002
AI639488	ESTs, moderate similarity to protein prf:1814460A (*H. sapiens*) 1814460A p53-associated protein (*Homo sapiens*)	0.68 ± 0.76	2.93 ± 1.23	↑ 4.3	0.0008
J05122	Benzodiazepin receptor	0.63 ± 0.35	2.51 ± 0.95	↑ 4.0	0.0007
X61654	CD63 antigen	0.46 ± 0.32	1.82 ± 0.79	↑ 3.9	0.0016
AI104781	Arachidonate 5-lipoxygenase activating protein	0.61 ± 0.42	2.38 ± 1.14	↑ 3.9	0.0027
AI169104	ESTs, weak similarity to protein sp:P02776 (*H. sapiens*) PLF4_HUMAN Platelet factor 4 precursor (PF-4)	0.55 ± 0.40	2.16 ± 1.03	↑ 3.9	0.0027
AI171962	Annexin 1	0.57 ± 0.39	1.88 ± 0.56	↑ 3.3	0.0001
X62951	*R. norvegicus* mRNA (pBUS19) with repetitive elements	0.89 ± 1.10	2.92 ± 1.69	↑ 3.3	0.0114
U02320	Neuregulin 1	0.69 ± 0.52	2.19 ± 0.59	↑ 3.2	<0.0001
AA900505	rhoB gene	0.78 ± 0.47	2.38 ± 0.61	↑ 3.1	<0.0001
M12919	Aldolase A	0.54 ± 0.23	1.66 ± 0.59	↑ 3.1	0.0008
AJ009698	Embigin	0.57 ± 0.37	1.74 ± 0.54	↑ 3.0	0.0002

TABLE 5
CONTINUED

GenBank Accession No.	Description	Mean ± SD of Fibrosis Score 0–1	Mean ± SD of Fibrosis Score 2–3	Fold Change	*p*-Value
Downregulated genes					
AA875523	*Rattus norvegicus* similar to Myosin light chain alkali, smooth-muscle isoform (MLC3SM) (LOC297831), mRNA	0.53 ± 0.26	1.52 ± 0.49	↑ 2.8	0.0005
M35300	Serine protease inhibitor, Kazal type 1	1.18 ± 1.49	3.29 ± 1.06	↑ 2.8	0.0008
AF017437	Integrin-associated protein	0.72 ± 0.36	1.96 ± 0.76	↑ 2.7	0.0020
AF020618	Myeloid differentiation primary response gene 116	0.89 ± 0.27	2.24 ± 1.32	↑ 2.5	0.0231
X52815	Unnamed protein product; cytoskeletal gamma-actin (AA 1-375); rat mRNA for cytoplasmic-gamma isoform of actin	0.63 ± 0.35	1.57 ± 0.41	↑ 2.5	0.0001
AA892851	*Rattus norvegicus* transcribed sequences	0.68 ± 0.28	1.63 ± 0.73	↑ 2.4	0.0073
AI233173	Expressed in nonmetastatic cells 1	0.74 ± 0.32	1.77 ± 0.52	↑ 2.4	0.0005
AA892373	Syntenin	0.75 ± 0.26	1.71 ± 0.78	↑ 2.3	0.0098
AA893584	*Rattus norvegicus* transcribed sequence with weak similarity to protein ref:NP_500967.1 (*C. elegans*)	0.76 ± 0.26	1.67 ± 0.51	↑ 2.2	0.0011
AI072634	Keratin complex 1, acidic, gene 18	0.86 ± 0.33	1.86 ± 0.57	↑ 2.2	0.0011
AI177096	ESTs, moderate similarity to protein pir:RTHUA (*H. sapiens*) RTHUA adenine phosphoribosyltransferase (EC 2.4.2.7)	0.76 ± 0.22	1.48 ± 0.33	↑ 1.9	0.0002
D17445	Tyrosine 3-monooxygenase/tryptophan 5-monooxygenase activation protein, eta polypeptide	0.74 ± 0.21	1.35 ± 0.26	↑ 1.8	<0.0001
AI639132	ESTs, similar to RIKEN cDNA 6720467C03 (predicted)	0.88 ± 0.28	1.48 ± 0.31	↑ 1.7	0.0005

Genes were ranked by fold change. Significance was calculated using *t*-test.

jected to damage, we believed that these genes might potentially provide information for clinical and medical studies based on our time course results.

Interactive and Knowledge-Sharing Website for Liver Necroinflammation and Fibrosis

To elucidate the detailed molecular signatures of liver necroinflammation and fibrosis, a large amount of sample is needed. Due to limited sample sources, our dataset only goes a small way towards a full understanding of liver fibrogenesis. To strengthen our dataset, a proprietary liver necroinflammatory and fibrosis-related gene expression data warehouse has been established, consisting of both ours and other publicly accessible microarray datasets, even though such integration remains difficult. We have downloaded the publicly accessible liver fibrosis microarray dataset (45) and manually keyed-in those genes reported to show differential expression patterns from liver fibrosis tissue samples. These collected datasets will serve as reference databases for us during further validation. All of these datasets have been deposited and reorganized at a website (http://LiverFibrosis.nchc.org.tw:8080/LF). We have deposited 24 microarray datasets (12 controls, 12 DMN treated) with four data formats: CEL, TXT, EXP, and DAT for free download and analysis. In addition, a necroinflammatory and fibrosis-related gene list from the public accessible microarray datasets and gene annotation is included at this website.

We implemented "softbots," or software agents, to collect scattered gene annotations either by mining data sources directly or by querying publicly accessible databases. For each liver fibrosis-related gene, the gene name, aliases, locus, gene ontology, protein–protein interactions, and various links to important bioinformatics and literature websites (PubMed, Uni Gene, GeneCards, GO, etc.) are displayed such that researchers may easily find the information they need. This results in an information-harvesting system that supports flexible storage and presentation and provides necessary accurate information to liver fibrosis researchers. The system supports both flexible storage and presentation. The result is an annotation engine that provides the precise information necessary for liver fibrosis research.

To organize the histopathological data from the control group and DMN group, a histopathological section has been established in same website. This website contains the 6-week time course dataset and each experimental week of the histopathological slices taken from 2–7 different rats. In addition, the biochemical data for each rat are also included in the view panel within the website.

DISCUSSION

Liver fibrosis represents a continuous disease spectrum characterized by an increase in total liver collagen and other matrix proteins that disrupt the archi-

TABLE 6
SUMMARY OF MICROARRAY DATASETS COMPARISON

GenBank Accession No.	Description	Microarray Dataset: 256 Genes	Rat*	Human†	Human‡	Mice§	Marker¶
AA859305	Tropomyosin isoform 6	↑				↑	
AA875523	Similar to 17,000 Da myosin light chain (LOC362816), mRNA	↑				↑	
AA892775	Lysozyme	↑				↑	
AF001898	Aldehyde dehydrogenase family 1, member A1	↑				↑	
AF023087	Early growth response 1	↑			↑	↑	
AF083269	Actin related protein 2/3 complex, subunit 1B	↑				↑	
AI072634	Keratin complex 1, acidic, gene 18	↑	↑				
AI169327	Tissue inhibitor of metalloproteinase 1	↑					↑
AI169370	Alpha-tubulin	↑	↑				
AI231292	Cystatin C	↑	↑				
J02962	Lectin, galactose binding, soluble 3	↑	↑				
J05122	Benzodiazepin receptor	↑	↑			↑	
L38615	Glutathione synthetase	↑				↑	
M12156	Heterogeneous nuclear ribonucleoprotein A1	↑				↑	
M12919	Aldolase A	↑				↑	
M37584	H2A histone family, member Z	↑				↑	
M58404	Thymosin, beta 10	↑	↑				
M60921	B-cell translocation gene 2, antiproliferative	↑				↑	
M63282	Activating transcription factor 3	↑			↑		
S72594	Tissue inhibitor of metalloproteinase type 2	↑					↑
U60882	Heterogeneous nuclear ribonucleoproteins methyltransferase-like 2 (*S. cerevisiae*)	↑			↓		
X02904	Glutathione *S*-transferase, pi 2	↑				↑	
X07944	Rat ornithine decarboxylase gene (EC 4.1.1.17)	↑				↑	
X54617	Myosin regulatory light chain	↑				↑	
X58465	Rat mRNA for ribosomal protein S5	↑	↑			↑	
X61654	CD63 antigen	↑				↑	
X62322	Granulin	↑				↑	
X70871	Cyclin G1	↑			↓		
AA799560	N-myc downstream-regulated gene 2	↓				↓	
AA799645	FXYD domain-containing ion transport regulator 1	↓		↓		↓	
AA892832	Fatty acid elongase 1	↓				↑	
AF080468	Glucose-6-phosphatase, transport protein 1	↓	↓				
AI013861	3-Hydroxyisobutyrate dehydrogenase	↓				↓	
AI177004	3-Hydroxy-3-methylglutaryl-coenzyme A synthase 1	↓				↓	
D00362	Esterase 2	↓				↑	
D13921	Acetyl-coenzyme A acetyltransferase 1	↓		↓			
D90109	Fatty acid Coenzyme A ligase, long chain 2	↓	↓				
J02592	Glutathione *S*-transferase Yb subunit	↓				↓	
J02791	Acetyl-coenzyme A dehydrogenase, medium chain	↓		↓		↓	
M00002	Apolipoprotein A-IV	↓	↓				
M11670	Catalase	↓		↓			
M12337	Phenylalanine hydroxylase	↓				↓	
M16235	Lipase, hepatic	↓				↓	
M26127	Cytochrome P450, 1a2	↓	↓				
M33648	3-Hydroxy-3-methylglutaryl-coenzyme A synthase 2	↓				↑	
M64755	Cysteine-sulfinate decarboxylase	↓				↓	
M67465	Hydroxy-delta-5-steroid dehydrogenase, 3 beta- and steroid delta-isomerase	↓				↓	
M77479	Solute carrier family 10, member 1	↓	↓	↓			
M89945	Rat farnesyl diphosphate synthase gene, exons 1-8	↓				↓	
S83279	Peroxisome proliferator-inducible gene	↓		↓			
U17697	Cytochrome P450, subfamily 51	↓				↓	
U94856	Paraoxonase 1	↓	↓			↓	
X06150	Glycine methyltransferase	↓				↓	
X12459	Arginosuccinate synthetase	↓	↓				

↑: Upregulation to control; ↓: downregulation to control.
*From Utsunomiya et al. (45).
†273 HCC-associated signatures. From Kim et al. (26).
‡283 Etiology-associated signatures. From Kim et al. (26).
§From White et al. (50).
¶From Friedman (13), Hayasaka and Sausho (19), and Iredale (23).

SUPPLEMENTAL TABLE 1
THE GENE EXPRESSION PATTERNS OF FIBROSIS MARKERS BY QUANTITATIVE REAL-TIME PCR AND MICROARRAY DATA

Markers	Description	Invasive Detection	Expression Stage	Qualitative RT-PCR*	Probe Set ID	Microarray Data*	Reference
Lox	Lysyl oxidase	yes	mRNA		S66184_s_at	↑	13
					rc_AA875582_at	↑	
					rc_AI102814_at	↓	
					rc_AI234060_s_at	↑	
P4h	Prolyl 4-hydroxylase	yes	mRNA		M21476_s_at	ND	13
					X02918_at	↓	
					X02918_g_at	ND	
					X78949_at	↑	
Tnc	Tenascin C	yes	mRNA		U09361_s_at	↑	13,19
					U09401_s_at	↓	
					U15550_at	↑	
Mmp2	Matrix metalloproteinase 2 (72 kDa type IV collagenase)	yes	mRNA		U65656_at	↑	13,19
					X71466_at	↓	
Mmp3	Matrix metalloproteinase 3	yes	mRNA	↑	X02601_at	↑	19
Timp1	Tissue inhibitor of metalloproteinase 1	yes	mRNA, protein	↑	rc_AI169327_at	↑	13,19,23
					rc_AI169327_g_at	↑	
Timp2	Tissue inhibitor of metalloproteinase type 2	yes	mRNA, protein	↑	S72594_s_at	↑	19,23
Col4	Collagen, type IV, alpha 3	yes	mRNA, protein		L47281_at	↓	13
Tgfb1	Transforming growth factor beta-1 gene	no	mRNA, protein	↑	X52498cds_at	↑	23
A2m	Alpha-2-macroglobulin	no	protein		X13983mRNA_at	↓	13
					M22670cds_g_at	↑	
					rc_AA900582_at	↑	
					rc_AI113046_at	↑	
Vtn	Vitronectin	no	protein		U44845_at	↓	19
Hp	Haptoglobin	no	protein		K01933_at	↓	13
Ggt	Gamma-glutamyl transpeptidase	no	protein	↑	M33822_at	↑	13
					X03518cds#3_s_at	↑	
Apoa	Apolipoprotein A	no	protein		M00001_i_at	↑	13
					M00002_at	↓	
					X03468_at	↓	

Genes were ranked by invasive detection.
*↑: upregulation to control; ↓: downregulation to control; ND: no different to control.

tecture of the liver and impair liver function (11,12). The progression of fibrosis in the liver is a response to necroinflammatory changes. The overall liver fibrosis process is a dynamic inflammation and repair, and has the potential to be resolved (23). In this study, we applied microarray analysis to continuously monitor the gene expression profile of DMN-induced liver fibrosis over 6 weeks. Classification based on histopathological gradings identified 256 liver damage-related genes and these could be divided into 44 and 62 features that acted as the best necroinflammatory and fibrosis discriminators. Moreover, data comparisons with other microarray datasets further elucidated the liver regeneration subgroups. To our knowledge, this is the first report to delineate the molecular portrait of liver fibrosis based on the process of necroinflammation, fibrosis, and liver regeneration over a time course. Interestingly, among the 256 liver damage-related genes, approximately half of them are not well annotated. In comparison with 39 well-known fibrosis markers, our study substantially increases the number of fibrosis signatures, although this inventory is not yet complete. Our data not only set the stage for a functional dissection of these liver fibrosis-related genes but also open up a new perspective on several uncharacterized novel genes linked to the human disease and provides potential targets for the rational development of therapeutic drugs.

Accumulation of data with respect to the expression profiles of liver specimens, histopathological data, and biochemical data will help us to understand the precise molecular mechanisms of necroinflammatory progression and liver hepatic bridging fibrosis. However, how to effectively utilize the vast amount of information gathered through this study remains

SUPPLEMENTAL TABLE 2
THE SIMILAR EXPRESSION GENES OF FIBROSIS MARKERS

Markers	GenBank ID	Gene Symbol	Gene Name	Pearson Correlation
Tissue inhibitor of metalloproteinase 1	S72594	Timp2	Tissue inhibitor of metalloproteinase type 2, TIMP-2	0.99
	M32062	Fcgr3	Fc receptor, IgG, low affinity III	0.99
	M76704	Mgmt	0^6-methylguanine-DNA methyltransferase	0.98
	M35300	Spink1	Serine protease inhibitor, Kazal type 1	0.98
	M58404	Tmsb10	Thymosin, beta 10	0.98
	AI171962	Anxa1	Annexin 1	0.97
	AB010635	Ces2	Carboxylesterase 2 (intestine, liver)	0.97
	M81855	Pgy1	P-glycoprotein/multidrug resistance 1	0.97
	J03627	S100a10	S-100 related protein, clone 42C	0.97
	X62952	Vim	Vimentin	0.97
Tissue inhibitor of metalloproteinase 2	AI169327	Timp1	Tissue inhibitor of metalloproteinase 1	0.99
	M32062	Fcgr3	Fc receptor, IgG, low affinity III	0.98
	M76704	Mgmt	0^6-methylguanine-DNA methyltransferase	0.98
	M81855	Pgy1	P-glycoprotein/multidrug resistance 1	0.98
	J02962	Lgals3	Lectin, galactose binding, soluble 3	0.98
	M58404	Tmsb10	Thymosin, beta 10	0.98
	M12156	Hnrpa1	Heterogeneous nuclear ribonucleoprotein A1	0.98
	M35300	Spink1	Serine protease inhibitor, Kazal type 1	0.98
	AA892775	Lyz	Lysozyme	0.97
	S76511	Bax	Bax=apoptosis inducer (rats, ovary, mRNA Partial, 402 nt)	0.97

a significant challenge. This is simply because gene annotation is scattered and its content is hard to update or improve. Therefore, it was imperative to design an information-harvesting infrastructure that supports flexible storage and presentation as well as providing a good content management environment. Using this study, we wish to cause a paradigm shift by providing a web-based service and by publishing organized information via semantic webs. Softbots, or software agents, are implemented to collect scattered gene annotations either by mining data sources directly or by querying publicly accessible databases. Because our website is an integrated biological information portal with the built-in online editing tools and versatile sharing mechanisms, we welcome other researchers who might want to contribute their liver fibrosis-related microarray and/or proteomics datasets into this public accessible website. Moreover, this website also hyperlinks to the newly established ECHO, the Encyclopedia of Hepatocellular Carcinoma Genes Online (http://ehco.nchc.org.tw), allowing geographically distant researchers to freely access these valuable genomic datasets. Expansion of this dataset is part of our continuing effort (by reviewing the literature) aimed at elucidating the transcriptome and it will easily allow the inclusion of additional gene expression data contributed by other investigators worldwide.

Among the necroinflammatory-associated genes, endothelial cell-specific molecule (*Esm1*) was overexpressed in DMN-treated samples. *Esm1* was originally identified in lung and kidney endothelial cells, where its expression is regulated by cytokines, especially interleukin-6 (IL-6) (6,49). The expression of *Esm1* is related to systemic inflammation in adipocytes and might play a role in the regulation of the inflammatory processes by a protein kinase C-mediated signal pathway (49). Based on a hepatobiliary disease study, vimentin (*Vim*), the cytoskeleton gene, was also found to be overexpressed in bile ductules and interlobular bile ducts. Moreover, vimentin shows a heterogeneous antigenic expression as intermediate filaments in biliary epithelial cells and may be related to proliferation and reorganization (38).

CD63, a transmembrane protein, is also one of our fibrosis gene signatures and is upregulated after DMN treatment. Hepatic stellate cells (HSC), also known as Ito cells, are now well known to be a key cellular element involved in the development of hepatic fibrosis. Following chronic injury, HSCs activate or differentiate into myofibroblast-like cells, acquiring contractile, proinflammatory, and fibrogenic properties (30,35,36). Activated HSCs migrate and accumulate at the sites of tissue repair, secreting large amounts of extracellular matrix proteins during the progression of fibrosis. Activated HSC have been identified as the major collagen (one of extracellular matrix proteins)-producing cells and an initiator of liver fibrosis when the liver is injured (4). It has been demonstrated that inhibition of CD63 will inhibit collagen secretion and HSC migration (32). It has been suggested that CD63 might be a novel diagnostic

marker for the injured liver. Moreover, in an alcoholic liver disease (ALD) study (43), Annexin A1 (*Anxa1*) was highly expressed after liver injury. A recent study has indicated that alcohol-initiated liver injury occurs via inflammation. ALD progression involves continuing liver injury, fibrosis, and impaired liver regeneration. It suggested that *Anxa1* might play a role in the progression of fibrosis.

Chronic inflammation and hepatic cell damage might provide the proliferation stimuli for the promotion of hepatocarcinogenesis (42). Proteomics analysis using human primary biliary cirrhosis and normal tissues indicated that SPP1 is also highly expressed in primary biliary cirrhosis and is involved in the formation of epithelioid granuloma (18). Recently, SPP1, which is a secreted matrix protein (33), has been identified as a lead gene for the HCC signature and it has been shown to be overexpressed in metastatic HCC. Moreover, SPP1-specific antibodies can block HCC cell invasion effectively in vitro and also inhibit pulmonary metastasis of HCC cells in nude mice (52). This data comparison supports the view that SPP1 not only acts as a potential therapeutic target for metastatic HCC, but also has the potential to be an early diagnostic marker for liver injury. Thus, it may be feasible in the future to diagnose patients with inflammation and fibrosis using only a serum sample (Fig. 4E).

The gene expression profiling carried out here provides a powerful and robust tool that is able to reveal molecular markers for liver damage at an early stage. In total, 256 genes were identified that were able to discriminate a liver damage situation from the normal situation; of these, 44 and 62 genes formed the best necroinflammatory and fibrosis discriminators, respectively. We have used these discriminators to rapidly screen potential Chinese herbs for the treatment of DMN-induced liver fibrosis. Among many herbs tested, one of them has shown a significant improvement in DMN-triggered liver damage as examined by histopathological and clinical biochemical analysis similar to those described in this study. More importantly, treatment with this newly identified herb could reverse more than 80% of these discriminators to the level of the normal control (data not shown). This result implies that identification of these discriminators not only allows them to serve as molecular classifiers that provide novel biological insights into the development of earlier liver damage but they can also help the development of new therapeutic drugs for liver disease.

ACKNOWLEDGMENTS

This work was supported in part by grants from the Liver Disease Prevention and Treatment Research Foundation, DOH (CCMP 94-RD-047) and National Health Research Institutes to L. J. Su, Taichung Veterans General Hospital and National Chi-Nan University (TCVGH-NCNU-927908 and 937903C) to S. L. Hsu, and National Health Research Institutes (MG-094-SP-01) to C. Y. F. Huang.

REFERENCES

1. Ala-Kokko, L.; Pihlajaniemi, T.; Myers, J. C.; Kivirikko, K. I.; Savolainen, E. R. Gene expression of type I, III and IV collagens in hepatic fibrosis induced by dimethylnitrosamine in the rat. Biochem. J. 244:75–79; 1987.
2. Al-Shahrour, F.; Diaz-Uriarte, R.; Dopazo, J. FatiGO: A web tool for finding significant associations of gene ontology terms with groups of genes. Bioinformatics 20:578–580; 2004.
3. Arthur, M. J.; Mann, D. A.; Iredale, J. P. Tissue inhibitors of metalloproteinases, hepatic stellate cells and liver fibrosis. J. Gastroenterol. Hepatol. 13(Suppl.): S33–38; 1998.
4. Bataller, R.; Brenner, D. A. Liver fibrosis. J. Clin. Invest. 115:209–218; 2005.
5. Bauer, M.; Schuppan, D. TGFbeta1 in liver fibrosis: Time to change paradigms? FEBS Lett. 502:1–3; 2001.
6. Bechard, D.; Meignin, V.; Scherpereel, A.; Oudin, S.; Kervoaze, G.; Bertheau, P.; Janin, A.; Tonnel, A.; Lassalle, P. Characterization of the secreted form of endothelial-cell-specific molecule 1 by specific monoclonal antibodies. J. Vasc. Res. 37:417–425; 2000.
7. Crabb, D. W. Recent developments in alcoholism: The liver. Recent Dev. Alcohol 11:207–230; 1993.
8. Day, C. P. Non-alcoholic steatohepatitis (NASH): Where are we now and where are we going? Gut 50: 585–588; 2002.
9. Dooley, S.; Delvoux, B.; Streckert, M.; Bonzel, L.; Stopa, M.; ten Dijke, P.; Gressner, A. M. Transforming growth factor beta signal transduction in hepatic stellate cells via Smad2/3 phosphorylation, a pathway that is abrogated during in vitro progression to myofibroblasts. TGFbeta signal transduction during transdifferentiation of hepatic stellate cells. FEBS Lett. 502: 4–10; 2001.
10. Fausto, N. Liver regeneration. J. Hepatol. 32:19–31; 2000.
11. Friedman, S. L. Seminars in medicine of the Beth Israel Hospital, Boston. The cellular basis of hepatic fibrosis. Mechanisms and treatment strategies. N. Engl. J. Med. 328:1828–1835; 1993.
12. Friedman, S. L. Molecular regulation of hepatic fibrosis, an integrated cellular response to tissue injury. J. Biol. Chem. 275:2247–2250; 2000.

13. Friedman, S. L. Liver fibrosis—from bench to bedside. J. Hepatol. 38(Suppl. 1):S38–53; 2003.
14. George, J.; Rao, K. R.; Stern, R.; Chandrakasan, G. Dimethylnitrosamine-induced liver injury in rats: The early deposition of collagen. Toxicology 156:129–138; 2001.
15. Gressner, A. M.; Weiskirchen, R.; Breitkopf, K.; Dooley, S. Roles of TGF-beta in hepatic fibrosis. Front. Biosci. 7:d793–807; 2002.
16. Haggerty, H. G.; Holsapple, M. P. Role of metabolism in dimethylnitrosamine-induced immunosuppression: A review. Toxicology 63:1–23; 1990.
17. Halliday, J. W.; Searle, J. Hepatic iron deposition in human disease and animal models. Biometals 9:205–209; 1996.
18. Harada, K.; Ozaki, S.; Sudo, Y.; Tsuneyama, K.; Ohta, H.; Nakanuma, Y. Osteopontin is involved in the formation of epithelioid granuloma and bile duct injury in primary biliary cirrhosis. Pathol. Int. 53:8–17; 2003.
19. Hayasaka, A.; Saisho, H. Serum markers as tools to monitor liver fibrosis. Digestion 59:381–384; 1998.
20. Iizuka, N.; Oka, M.; Yamada-Okabe, H.; Mori, N.; Tamesa, T.; Okada, T.; Takemoto, N.; Hashimoto, K.; Tangoku, A.; Hamada, K.; Nakayama, H.; Miyamoto, T.; Uchimura, S.; Hamamoto, Y. Differential gene expression in distinct virologic types of hepatocellular carcinoma: Association with liver cirrhosis. Oncogene 22:3007–3014; 2003.
21. Imbert-Bismut, F.; Ratziu, V.; Pieroni, L.; Charlotte, F.; Benhamou, Y.; Poynard, T. Biochemical markers of liver fibrosis in patients with hepatitis C virus infection: A prospective study. Lancet 357:1069–1075; 2001.
22. Iredale, J. P. Tissue inhibitors of metalloproteinases in liver fibrosis. Int. J. Biochem. Cell Biol. 29:43–54; 1997.
23. Iredale, J. P. Cirrhosis: New research provides a basis for rational and targeted treatments. Br. Med. J. 327: 143–147; 2003.
24. Ishak, K.; Baptista, A.; Bianchi, L.; Callea, F.; De Groote, J.; Gudat, F.; Denk, H.; Desmet, V.; Korb, G.; MacSween, R. N.; Phillips, M. J.; Portmann, B. G.; Poulsen, H.; Scheuer, P. J.; Schmid, M.; Thaler, H. Histological grading and staging of chronic hepatitis. J. Hepatol. 22:696–699; 1995.
25. Jezequel, A. M.; Mancini, R.; Rinaldesi, M. L.; Macarri, G.; Venturini, C.; Orlandi, F. A morphological study of the early stages of hepatic fibrosis induced by low doses of dimethylnitrosamine in the rat. J. Hepatol. 5:174–181; 1987.
26. Kim, J. W.; Ye, Q.; Forgues, M.; Chen, Y.; Budhu, A.; Sime, J.; Hofseth, L. J.; Kaul, R.; Wang, X. W. Cancer-associated molecular signature in the tissue samples of patients with cirrhosis. Hepatology 39:518–527; 2004.
27. Knodell, R. G.; Ishak, K. G.; Black, W. C.; Chen, T. S.; Craig, R.; Kaplowitz, N.; Kiernan, T. W.; Wollman, J. Formulation and application of a numerical scoring system for assessing histological activity in asymptomatic chronic active hepatitis. Hepatology 1: 431–435; 1981.
28. Llovet, J. M.; Bustamante, J.; Castells, A.; Vilana, R.; Ayuso Mdel, C.; Sala, M.; Bru, C.; Rodes, J.; Bruix, J. Natural history of untreated nonsurgical hepatocellular carcinoma: rationale for the design and evaluation of therapeutic trials. Hepatology 29:62–67; 1999.
29. Lopez-De Leon, A.; Rojkind, M. A simple micromethod for collagen and total protein determination in formalin-fixed paraffin-embedded sections. J. Histochem. Cytochem. 33:737–743; 1985.
30. Marra, F.; Arrighi, M. C.; Fazi, M.; Caligiuri, A.; Pinzani, M.; Romanelli, R. G.; Efsen, E.; Laffi, G.; Gentilini, P. Extracellular signal-regulated kinase activation differentially regulates platelet-derived growth factor's actions in hepatic stellate cells, and is induced by in vivo liver injury in the rat. Hepatology 30:951–958; 1999.
31. Marvanova, M.; Menager, J.; Bezard, E.; Bontrop, R. E.; Pradier, L.; Wong, G. Microarray analysis of nonhuman primates: Validation of experimental models in neurological disorders. FASEB J. 17:929–931; 2003.
32. Mazzocca, A.; Carloni, V.; Sciammetta, S.; Cordella, C.; Pantaleo, P.; Caldini, A.; Gentilini, P.; Pinzani, M. Expression of transmembrane 4 superfamily (TM4SF) proteins and their role in hepatic stellate cell motility and wound healing migration. J. Hepatol. 37:322–330; 2002.
33. Medico, E.; Gentile, A.; Lo Celso, C.; Williams, T. A.; Gambarotta, G.; Trusolino, L.; Comoglio, P. M. Osteopontin is an autocrine mediator of hepatocyte growth factor-induced invasive growth. Cancer Res. 61:5861–5868; 2001.
34. Michalopoulos, G. K.; DeFrances, M. C. Liver regeneration. Science 276:60–66; 1997.
35. Milani, S.; Herbst, H.; Schuppan, D.; Kim, K. Y.; Riecken, E. O.; Stein, H. Procollagen expression by nonparenchymal rat liver cells in experimental biliary fibrosis. Gastroenterology 98:175–184; 1990.
36. Milani, S.; Herbst, H.; Schuppan, D.; Surrenti, C.; Riecken, E. O.; Stein, H. Cellular localization of type I III and IV procollagen gene transcripts in normal and fibrotic human liver. Am. J. Pathol. 137:59–70; 1990.
37. Mirsalis, J. C.; Butterworth, B. E. Detection of unscheduled DNA synthesis in hepatocytes isolated from rats treated with genotoxic agents: An in vivo-in vitro assay for potential carcinogens and mutagens. Carcinogenesis 1:621–625; 1980.
38. Nakanuma, Y.; Kono, N. Expression of vimentin in proliferating and damaged bile ductules and interlobular bile ducts in nonneoplastic hepatobiliary diseases. Mod. Pathol. 5:550–554; 1992.
39. Okita, K.; Sakaida, I.; Hino, K. Current strategies for chemoprevention of hepatocellular carcinoma. Oncology 62(Suppl. 1):24–28; 2002.
40. Rogers, A. E.; Newberne, P. M. Animal model: Fatty liver and cirrhosis in lipotrope-deficient male rats. Am. J. Pathol. 73:817–820; 1973.

41. Schuppan, D.; Krebs, A.; Bauer, M.; Hahn, E. G. Hepatitis C and liver fibrosis. Cell Death Differ. 10(Suppl. 1):S59–67; 2003.
42. Seow, T. K.; Liang, R. C.; Leow, C. K.; Chung, M. C. Hepatocellular carcinoma: from bedside to proteomics. Proteomics 1:1249–1263; 2001.
43. Seth, D.; Leo, M. A.; McGuinness, P. H.; Lieber, C. S.; Brennan, Y.; Williams, R.; Wang, X. M.; McCaughan, G. W.; Gorrell, M. D.; Haber, P. S. Gene expression profiling of alcoholic liver disease in the baboon (*Papio hamadryas*) and human liver. Am. J. Pathol. 163:2303–2317; 2003.
44. Tan, A. C.; Gilbert, D. Ensemble machine learning on gene expression data for cancer classification. Appl. Bioinformatics 2:S75–83; 2003.
45. Utsunomiya, T.; Okamoto, M.; Hashimoto, M.; Yoshinaga, K.; Shiraishi, T.; Tanaka, F.; Mimori, K.; Inoue, H.; Watanabe, G.; Barnard, G. F.; Mori, M. A gene-expression signature can quantify the degree of hepatic fibrosis in the rat. J. Hepatol. 41:399–406; 2004.
46. Vickers, A. E.; Saulnier, M.; Cruz, E.; Merema, M. T.; Rose, K.; Bentley, P.; Olinga, P. Organ slice viability extended for pathway characterization: An in vitro model to investigate fibrosis. Toxicol. Sci. 82:534–544; 2004.
47. Waring, J. F.; Ciurlionis, R.; Jolly, R. A.; Heindel, M.; Ulrich, R. G. Microarray analysis of hepatotoxins in vitro reveals a correlation between gene expression profiles and mechanisms of toxicity. Toxicol. Lett. 120:359–368; 2001.
48. Waring, J. F.; Jolly, R. A.; Ciurlionis, R.; Lum, P. Y.; Praestgaard, J. T.; Morfitt, D. C.; Buratto, B.; Roberts, C.; Schadt, E.; Ulrich, R. G. Clustering of hepatotoxins based on mechanism of toxicity using gene expression profiles. Toxicol. Appl. Pharmacol. 175:28–42; 2001.
49. Wellner, M.; Herse, F.; Janke, J.; Gorzelniak, K.; Engeli, S.; Bechart, D.; Lasalle, P.; Luft, F. C.; Sharma, A. M. Endothelial cell specific molecule-1—a newly identified protein in adipocytes. Horm. Metab. Res. 35: 217–221; 2003.
50. White, P.; Brestelli, J. E.; Kaestner, K. H.; Greenbaum, L. E. Identification of transcriptional networks during liver regeneration. J. Biol. Chem. 280:3715–3722; 2005.
51. Wu, J. C.; Chen, T. Y.; Yu, C. T.; Tsai, S. J.; Hsu, J. M.; Tang, M. J.; Chou, C. K.; Lin, W. J.; Yuan, C. J.; Huang, C. Y. Identification of V23RalA-Ser194 as a critical mediator for Aurora-A-induced cellular motility and transformation by small pool expression screening. J. Biol. Chem. 280:9013–9022; 2005.
52. Ye, Q. H.; Qin, L. X.; Forgues, M.; He, P.; Kim, J. W.; Peng, A. C.; Simon, R.; Li, Y.; Robles. A. I.; Chen, Y.; Ma, Z. C.; Wu, Z. Q.; Ye, S. L.; Liu, Y. K.; Tang, Z. Y.; Wang, X. W. Predicting hepatitis B virus-positive metastatic hepatocellular carcinomas using gene expression profiling and supervised machine learning. Nat. Med. 9:416–423; 2003.